Artificial metallo-proteins for photocatalytic water splitting: stability and activity in artificial photosynthesis

Opdam, L.V.

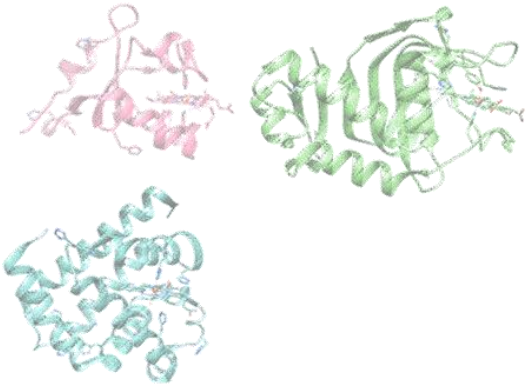

CHAPTER 1

INTRODUCTION

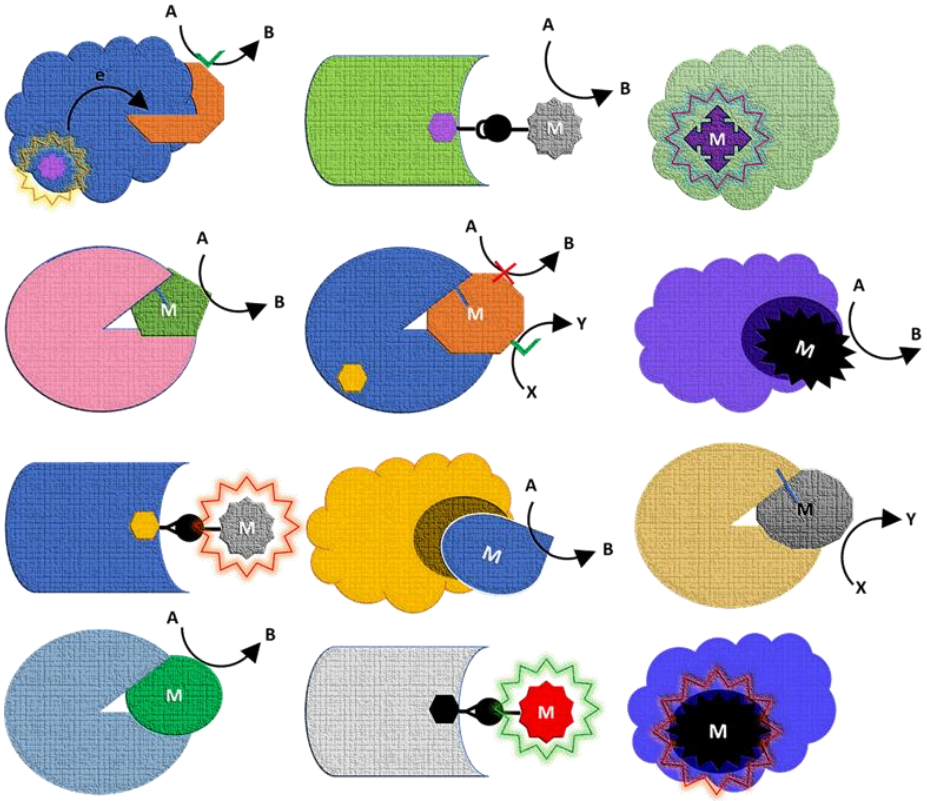

1 WATER SPLITTING

To combat global warming, an alternative to fossil fuels urgently needs to be found [1]. Compared to electricity, liquid fuels have great advantages in particular for transport and storage, and with that, for use in transportation and heavy industries [2]. Both the production of dihydrogen- and carbon-based fuels are currently being investigated, which requires the reduction either of protons or of CO_2 [2]–[5]. In either case, a source of electrons is needed; water is usually considered the most sustainable source of electrons, as it is widely available on earth and no harmful side products are produced upon water oxidation, only O_2 [6], [7]. In this thesis, we focussed on the preparation and study of artificial proteins for water oxidation (Eq. 1) and dihydrogen evolution (Eq. 2). Both reactions are defined by the two half-reactions:

$$2H_2O \rightarrow O_2 + 4e^- + 4H^+ \quad 1$$

$$2H^+ + 2e^- \rightarrow H_2 \quad 2$$

When both half-reactions can be coupled, water splitting is obtained, which is considered a highly attractive approach to generating green dihydrogen from renewable sources: sunlight and water [6], [8].

2 WATER OXIDATION IN NATURE (PSII)

Water oxidation (WO) is a kinetically and thermodynamically demanding reaction that requires catalysis to occur [9]. In nature, it is exclusively performed by photosystem II (PSII) [10]–[16]. The active core of PSII (Fig. 1H), defined as the set of proteins and cofactors minimally required to be able to perform water oxidation, consists of an inorganic manganese cluster, a protein heterodimer consisting of subunits D1 and D2, and the chlorophyll-containing proteins CP43 and CP47 [17]. Some isoforms of the D1 subunit have been found in cyanobacteria [18], but the remaining components of the active core have remained conserved throughout billions of years of evolution in diverse species, forming nature's only solution to the challenge of water oxidation [14]. CP43 and CP47 serve as light-harvesting antennae, in the full system transferring excitation energy from peripheral antenna systems to the reaction centre [17]. Subunits D1 and D2 hold most of the redox active cofactors in place, including the manganese cluster Mn_4CaO_5 [19]. The role of subunits D1 and D2 also lies in tuning the cofactors such that their electronically excited states can be transformed into charge-separated

states for water oxidation [19]. The manganese cluster is the cofactor through which catalytic water oxidation takes place [20]. It consists of three manganese ions forming the corners of an irregular cube together with a calcium atom and 4 oxygens. It is completed by another oxygen, 4 additional water molecules, and one manganese centre outside the cube [21]. Light energy captured by light-harvesting antenna systems is transferred to chlorophyll pair P680 in the reaction centre, where charge separation occurs [22]. The resulting P680 radical ion has a redox potential of +1.25 V^{NHE} [23], and the liberated electrons are transferred to pheophytin and then to the plastoquinone cofactors. P680 is located in between two tyrosine residues, Y161 from D1 and Y160 from D2. However, due to the precise tuning of the redox potential on each tyrosine the hole is transferred to Y161 from D1 only [20], [22], [24]. This hole transfer leads to oxidation of the manganese cluster, and through a series of absorbed photons, the cluster cycles through 4 S-states (S_1 through S_4), referring to the number of oxidizing equivalents present in the cluster, so that 4 electrons are ultimately liberated from 2 water molecules, releasing one molecule of dioxygen [14], [20]. The manganese cluster of PSII has a typical turnover frequency (*TOF*) of 100-400 s^{-1} [25].

Phototrophic organisms are often exposed to variable light conditions and a sudden increase in light exposure can lead to the formation of reactive oxygen species (ROS) that can damage the photosynthetic machinery leading to photoinhibition [26]. To prevent this inhibition, several non-photochemical quenching (NPQ) mechanisms have evolved. The fast NPQ mechanism is excitation energy quenching (qE), which acts on the light-harvesting antenna and involves the protein Photosystem II Subunit S (PSBS) in mosses and vascular plants and Light-Harvesting Complex Stress-Related (LHCSR) proteins in mosses and algae [26]–[28]. Another NPQ component related to photo-inhibition, termed qI, involves a light-dependent decrease of PSII activity, allowing efficient self-repair of damaged PSII. Self-repair involves the partial replacement of damaged PSII sites, especially the D1 protein where the actual WO takes place. Complete replacement of D1 subunit of PSII is a regular occurrence in natural photosynthesis, the half-life is strongly dependent on the light conditions and can be as little as 30 min under moderate light conditions [18], [29]–[31].

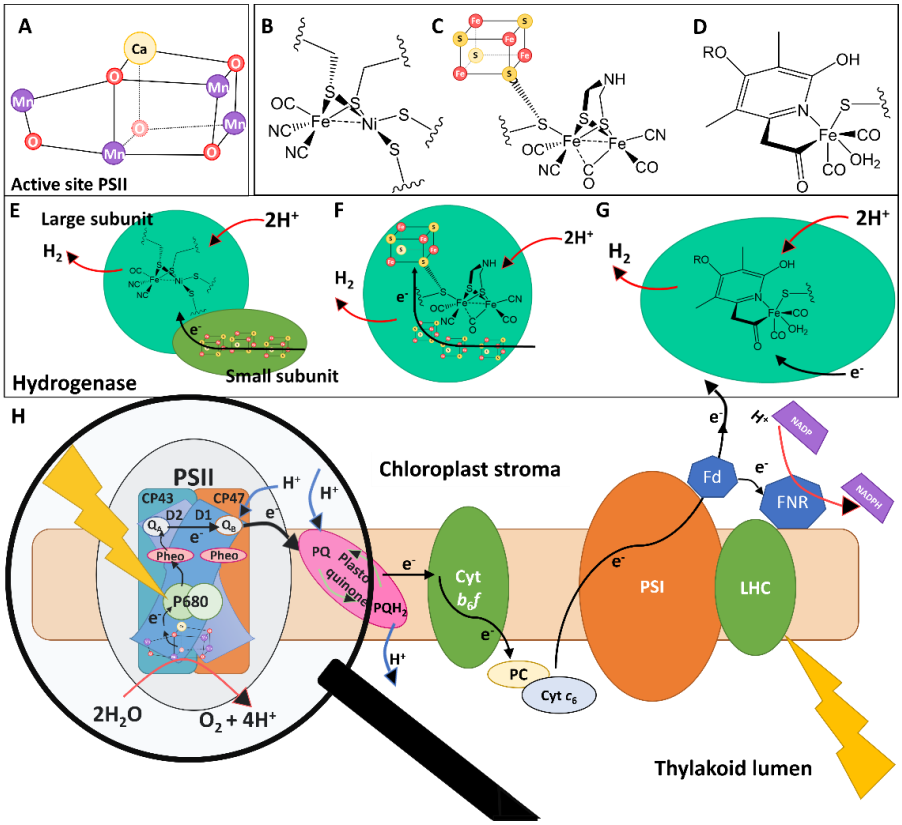

*Figure 1: In **A** the active site manganese cluster of PSII is shown, **B** the active site of [NiFe]-hydrogenase, **C** the active site of [FeFe]-hydrogenase, **D** the active site of [Fe]-hydrogenase, **E** a schematic of [NiFe]-hydrogenase , **F** a schematic of [FeFe]-hydrogenase, **G** a schematic of [Fe]-hydrogenase, **H** Electron transfer upon light excitation of PSI and PSII, leading to production of NADPH via ferredoxin (FNR) or of H_2 via hydrogenase as shown in **E-G**.*

3 H^+/H_2 CONVERSION IN NATURE

Under anaerobic conditions, microalgae and cyanobacteria can switch to dihydrogen production using an enzyme called hydrogenase [32]–[34]. While so-called uptake hydrogenases [35] only convert H_2 to H^+, some hydrogenases may also convert H^+ into H_2 when presented with electron donors: these proteins are called reversible hydrogenases [35]–[37]. H_2 is consumed by organisms to acquire energy, while its production can be used

to eliminate excess reducing equivalents. Hydrogenases can be divided into 3 classes based on their cofactor: the [NiFe] (Fig. 1B, E), [FeFe] (Fig. 1C, F), and [Fe] (Fig. 1D, G) hydrogenases [38], [39].

The [NiFe] class consists of a broad range of multi-subunit proteins consisting minimally of a large subunit, containing the [NiFe] cluster which forms the active site, and a small subunit, containing many [FeS] clusters serving as an electron relay [36], [40]. Most often nickel is coordinated by four cysteine thiol ligands, while iron is coordinated in an octahedral manner with CO and CN^- ligands, further sharing two thiol ligands with Ni (Fig. 1B) [36]. H_2 is heterolytically cleaved on the [NiFe] cluster, leading initially to the formation of a proton that is released and a hydride that coordinates in a bridging manner to the cluster. One hydride electron is transferred to nickel, which leads to the release of a second H^+ [36], the second hydride electron is transported by a *b*-type cytochrome to menaquinone [41]. To reinitialize the system the electron from nickel is released to menaquinone *via* the same route (Fig. 2B) [41].

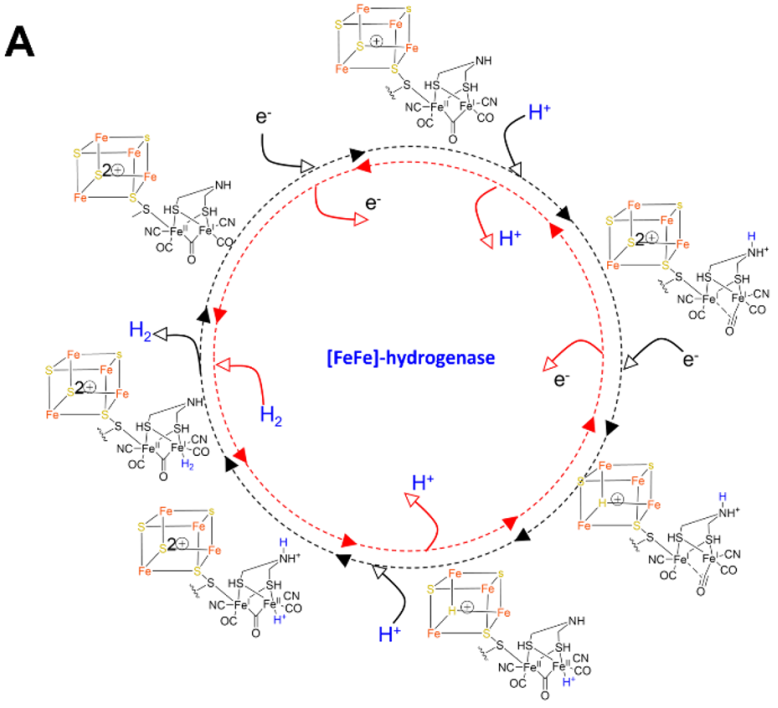

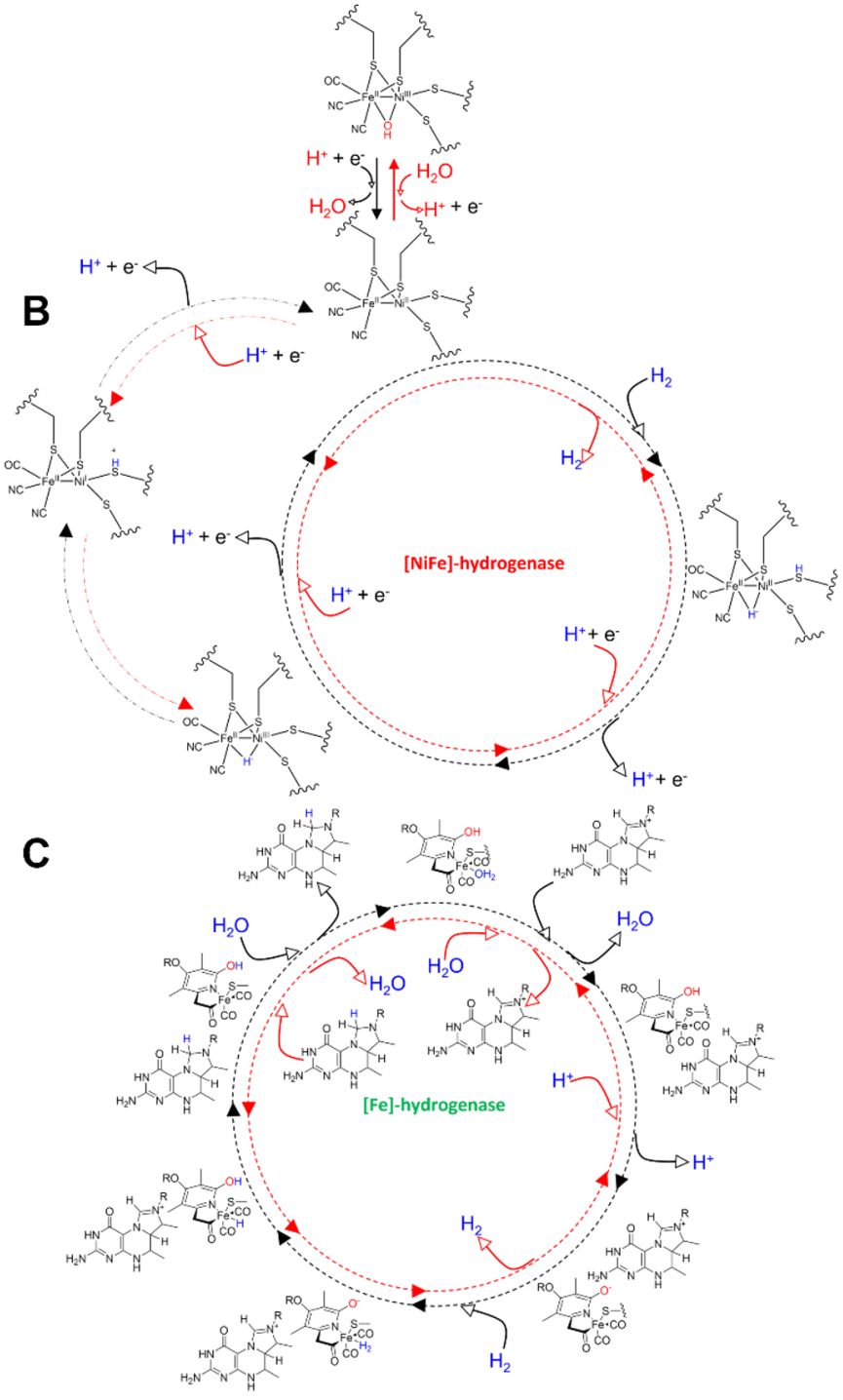
B
[NiFe]-hydrogenase
C
[Fe]-hydrogenase

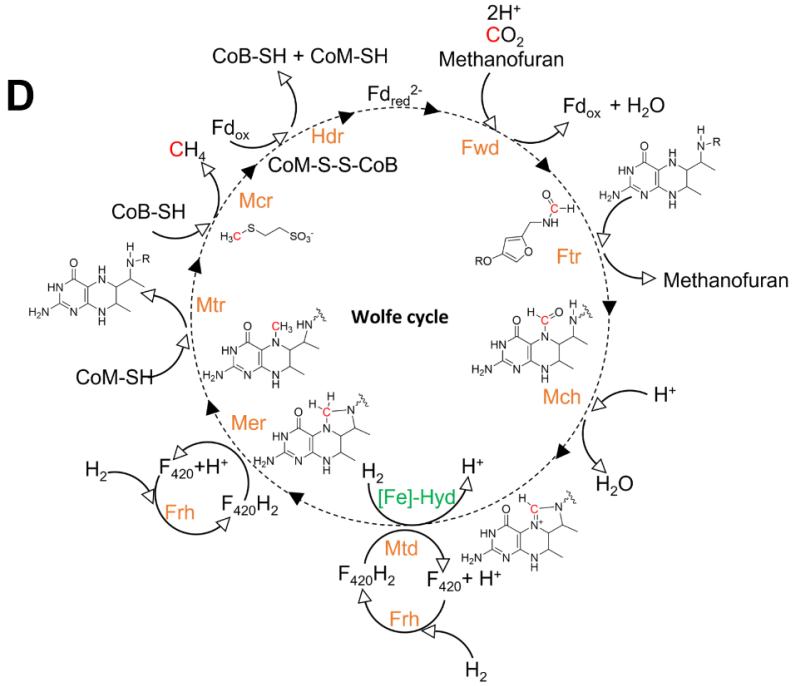

Figure 2: ***A-C*** *The mechanisms for the three types of hydrogenases with the two directions of their catalysis indicated with* ***black*** *and* ***red*** *arrows.* ***A*** *The putative mechanism of [FeFe]-hydrogenase involving oxidation of the iron sulphur and [FeFe] clusters* [42], [43]. ***B*** *The mechanism of dihydrogen oxidation by [NiFe]-hydrogenase including an initial step to convert oxidized [NiFe]-hydrogenase into its active form* [44]–[46]. ***C*** *The catalytic cycle of [Fe]-hydrogenase* [47] *in which the* N^5*,* N^{10}*-methenyl-tetrahydromethanophterin cofactor plays a major role.* ***D*** *The Wolfe cycle to convert* CO_2 *into* CH_4 [48]–[50]*, which is linked to [Fe]-hydrogenase ([Fe]-Hyd,* ***green****) activity. The Wolfe cycle further includes the following enzymes: ferredoxin in reduced or oxidized form (*Fd_{red}*/*Fd_{ox}*), formylmethanofuran dehydrogenase (fwd), tetrahydromethanopterin (H4MPT) formyltransferase (Ftr), methenyl-H4MPT cyclohydrolase (Mch), methylene-*H_4*MPT dehydrogense (Mtd),* F_{420}*-reducing hydrogenase (Frh), methylene-*H_4*MPT reductase (Mer), methyl-H4MPT:CoM methyltransferase (Mtr), methyl-coenzyme M reductase (Mcr), and heterodisulfide reductase (Hdr) in* ***orange****.*

In contrast to [NiFe] hydrogenases [FeFe] hydrogenases are usually monomeric. Each Fe in the [FeFe] cluster is hexacoordinated (Fig. 1C): the

coordinated ligands include a cysteine thiol ligand further linked to an [4Fe-4S] cluster, CO, CN^- and a bridging azadithiolate, the two iron centres share three ligands [51]–[53]. The mechanism of this type of hydrogenase is under investigation, but it involves changes in the oxidation state of both the [FeFe] and the [4Fe-4S] clusters to allow for the storage of 2 electrons (Fig. 2A) [54].

Finally, the [Fe] class of hydrogenases have a markedly different activity compared with the [FeFe] or [NiFe] hydrogenases, as they play a role in the Wolfe cycle for reduction of CO_2 to CH_4 using the reduction of the N^5-, N^{10}-methenyl-tetrahydromethanophterin cofactor catalysed by an Fe-guanylylpyridinol cofactor (Fig. 2C and D). The iron in the Fe-guanylylpyridinol cofactor is hexacoordinated, with 2 positions originating from the guanylylpyridinol group and the remainder being CO, H_2O, and cysteine (Fig. 1D). Here the heterolytic cleavage of H_2 takes place on CO_2 rather than on iron, which instead acts as a hydride acceptor [36], [55]–[57]. These three markedly different dihydrogen evolution strategies all use earth abundant metals. They may serve as an inspiration for the development of artificial catalysts [50]; their direct application, however, is impractical due to their strong sensitivity to the presence of dioxygen [6].

4 ARTIFICIAL PHOTOSYNTHESIS

In artificial photosynthesis the dihydrogen evolution and water oxidation reactions from (equations 1 and 2) are often optimized separately. The components of an artificial system for homogeneous photocatalytic water oxidation or dihydrogen evolution are a dihydrogen evolution or water oxidation catalyst (HEC or WOC), a photosensitizer (PS), and a sacrificial donor (SD) or acceptor (SA), respectively, which replaces the other half-reaction. For dihydrogen evolution, an electron relay such as methyl viologen (MV) may also be added, which modifies the kinetics of the reaction. In Fig. 3 a schematic representation of the reactions between the different components of a homogeneous photocatalytic water oxidation system (Fig. 3A) and of a dihydrogen evolution system (Fig. 3B) are shown. For the water oxidation reaction, catalyst oxidation can be driven by $PS^{+\bullet}$, while for the dihydrogen evolution reaction catalyst reduction is often driven by $PS^{-\bullet}$ (Fig. 3B). Alternatively, it can be driven directly by the excited photosensitizer *PS, followed by electron transfer to the sacrificial electron acceptor or from the donor (Fig. 3C). Water oxidation is considered the more challenging of the

two half-reactions of water splitting, both thermodynamically and kinetically [24].

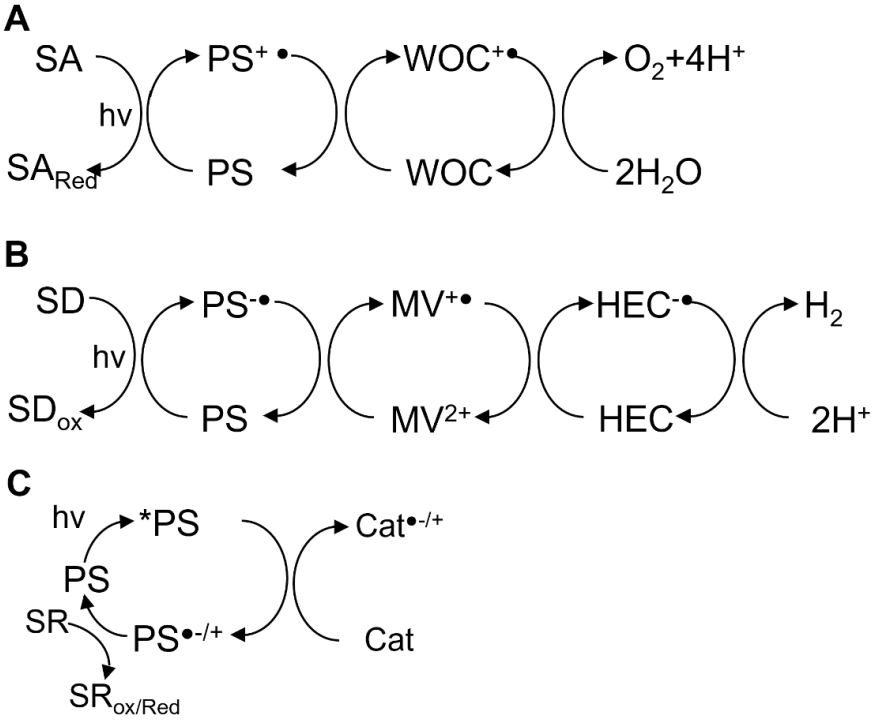

*Figure 3: Water oxidation driven by a photosensitizer (PS) and sacrificial acceptor (SA) (**A**), Hydrogen evolution driven by a photosensitizer and sacrificial donor (SD) via a common electron relay, here methyl viologen (MV) (**B**). In **C** the mechanism in which the photosensitizer excited state *PS can react with the catalyst is shown.*

Many synthetic catalysts with strong activity for water oxidation have been produced [10]–[13], [24], [58]–[62], but their applicability continues to be limited by their instability notably in photocatalytic conditions [63]. The best water oxidation catalysts contain ruthenium or iridium metal centres, though recently cobalt-based catalysts have been reported [10]–[13], [58]–[67]. Photocatalytic water oxidation is most commonly sensitized by $[Ru(bpy)_3]^{2+}$ with the sacrificial acceptor disodium peroxodisulphate ($Na_2S_2O_8$) [10]–[13], [58]–[67]. A drawback of this system is that $[Ru(bpy)_3]^{2+}$ is unstable under irradiation in the presence of a sacrificial acceptor, with oxidation of the bipyridyl ligands of the $[Ru(bpy)_3]^{3+}$ intermediate leading to the formation of

a poorly active, dimeric water oxidation catalyst called the “blue dimer” [68]. The Jablonski diagram of $[Ru(bpy)_3]^{2+}$ is shown in Fig. 4. $[Ru(bpy)_3]^{2+}$ can be excited by visible light (typically around 450 nm) to its singlet metal-to-ligand charge transfer (^{1}MLCT) excited state, from which it is quickly converted *via* intersystem crossing to the triplet state (^{3}MLCT). The lifetime of this excited state is relatively long, in the order of 580 ns in water at 25 °C [69], which allows it to react with a catalyst or sacrificial reagent in a bimolecular process, as detailed in Fig. 3, to transfer electrons.

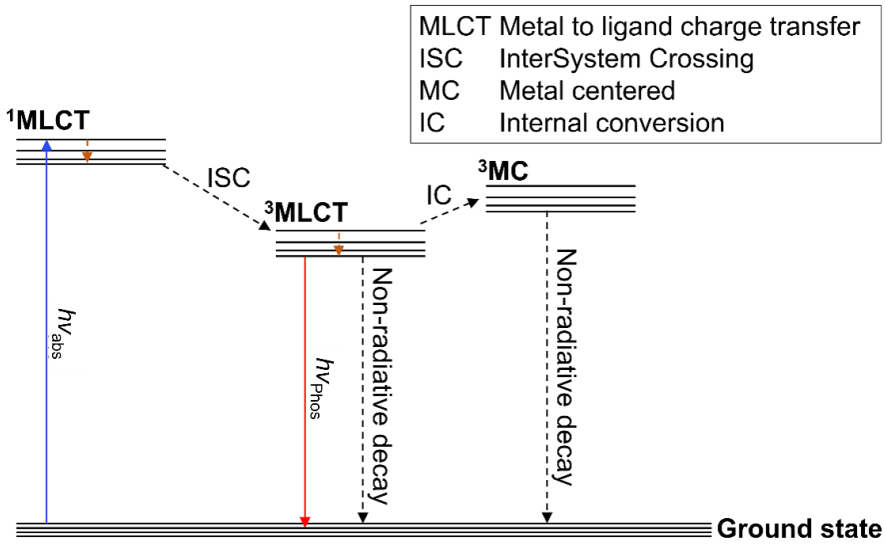

Figure 4: The Jablonski diagram of $[Ru(bpy)_3]^{2+}$ with interrupted lines indicating non-radiative processes. From left to right the singlet metal-to-ligand charge transfer excited state (^{1}MLCT), triplet metal-to-ligand charge transfer excited state (^{3}MLCT), and triplet metal-centered excited state (^{3}MC) are shown, with in between intersystem crossing (ISC) and internal conversion (IC).

Water oxidation catalysts generally operate via one of the two following mechanisms: the water nucleophilic attack (WNA, Fig. 5A) or the radical coupling mechanism (I2M, Fig. 5B). In WNA a metal oxo species, M=O, is attacked by water that acts as a nucleophile, forming a metal-peroxo species (M-O-O-H); in I2M dimerization of two metal oxo species M=O occurs to form a dimer M-O-O-M and thus an O-O bond, which finally releases O_2.

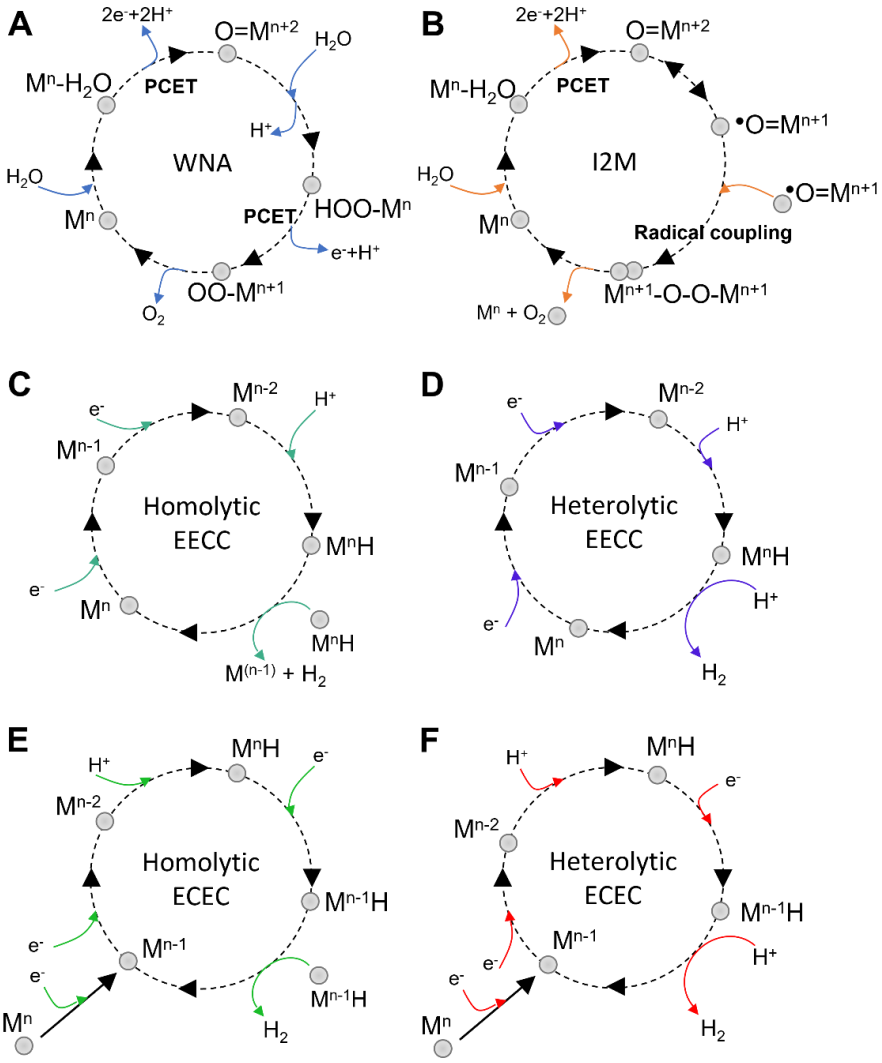

*Figure 5: Water oxidation via water nucleophilic attack (WNA, **A**) or the radical coupling mechanism (I2M, **B**). The metal catalyst (M with initial oxidation state n) is represented by a grey sphere, proton-coupled electron transfer (PCET) steps are indicated explicitly. Hydrogen evolution via the EECC (E = one-electron reduction, C = chemical protonation) (**C, D**) or ECEC (**E, F**) mechanism. Following either the homolytic (**C, E**) or the heterolytic (**D, F**) route.*

Catalysts for dihydrogen evolution are generally based on noble metals, *e.g.,* colloidal platinum, rhodium, ruthenium, and rhenium, though here too an important effort has been made to use earth-abundant metals or metal-free catalysts [70]–[73]. Dihydrogen evolution catalysis can typically be photosensitized by $[Ru(bpy)_3]^{2+}$, or soluble zinc porphyrin derivatives using sacrificial donors such as triethanolamine (TEOA), ethylenediaminetetraacetic acid (EDTA), or ascorbate, often (but not always) in combination with an electron relay such as methyl viologen (Fig. 3B) [73]–[75]. In Fig. 5 C-F the general mechanisms of dihydrogen evolution catalysis are shown. Figs. 5C-5D depicts the EECC mechanism, in which E stands for one-electron reduction and C for chemical protonation; Fig. 5E-5F depicts the ECEC mechanism. Within either category, the homolytic mechanism (Fig. 5C, 5D) hypothesizes that dihydrogen release involves the interaction of two MH complexes, while the heterolytic mechanism (Fig. 5E, F) postulates that dihydrogen release is accomplished by reaction of MH with an H^+ [70].

5 ARTIFICIAL METALLOENZYMES

Over the course of evolution, numerous enzymes have evolved, approximately half of which are metalloproteins [76]. The catalytic properties of their metal cofactors are carefully tuned by the protein environment, which is also called the second coordination sphere. This second coordination sphere often leads to improved specificity compared to small molecule catalysts; both in reactant selectivity and reaction product formation [77]. The protein second coordination sphere further allows complex chemical reactions to be performed at neutral pH, low pressures, and room temperature [78]. The fine-tuning opportunity that results from the existence of such a second coordination sphere in metalloenzymes has led to the development of artificial metalloenzymes (ArMs): catalytically active enzymes prepared from a non-native, often artificial metal cofactor, built into a protein scaffold [79]–[82]. A major strength of ArMs is the possibility to optimize them using directed evolution, which is a very powerful and fast method to improve their catalytic activity and stability, even when the understanding of the structure function relationship is not complete [83]–[87].

ArMs can be created via two routes: the restructuring route (Fig. 6A) focuses on the use of site-directed mutagenesis and directed evolution to modify the activity of existing metalloproteins, while the re-composition route (Fig. 6B-D) involves the introduction of a novel metal cofactor [77]. This route can be further divided based on how the non-native metal complex is introduced into the protein scaffold. Three ways can be distinguished: supramolecular (Fig. 6B) [88], dative (Fig. 6C) [89], [90], or covalent attachment (Fig. 6D) [79], [81], [91], [92]. Examples of the supramolecular attachment strategy are the binding of a catalyst to the protein streptavidin *via* a biotin linker, for which avidin shows high binding activity,[80], [93], [94] as well as binding to (bovine) serum albumin, which shows strong hydrophobic interaction with many types of molecules [91], [95]–[99]. The dative strategy involves the coordination of a metal by the protein, which then serves as a ligand. This strategy consists of the introduction of new metal ions or the replacement of a naturally occurring metal centre by another type of metal ion, for example when zinc is replaced by copper [79]. Sometimes entire cofactors can be replaced, such as haem that can be exchanged for other types of porphyrins [100]–[103]. Finally, the covalent attachment strategy can be used to create a novel, specific binding site in a protein, for example by introducing a cysteine residue to which *e.g.,* a maleimide [104]–[107] or methane thiosulfonate [108], [109] can be bound. Non-natural amino acids can also be used to create covalent attachment sites, for example to permit click chemistry [110], [111].

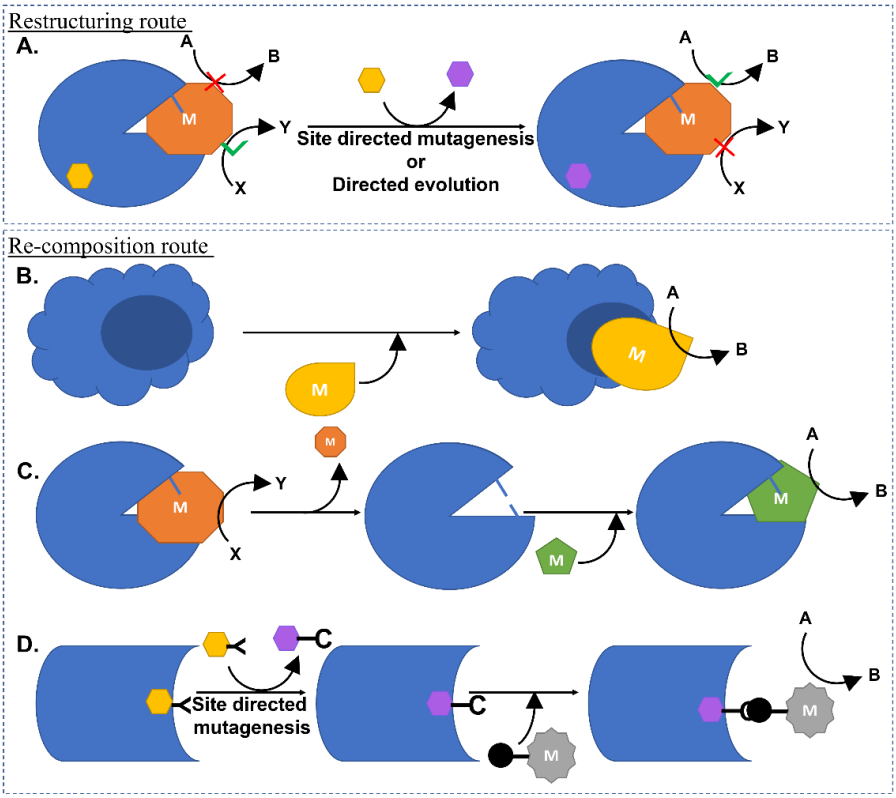

*Figure 6: Preparation of ArMs from protein scaffolds via the restructuring route (**A**) or via the re-composition route (**B-D**). The re-composition route is subdivided into the supramolecular (**B**), dative (**C**) and covalent (**D**) strategies. In each case the protein scaffold is shown in blue, the metal complexes in various shapes with an M in the centre. Mutations to the protein are shown with the exchange of a yellow hexagon to a purple hexagon, in **D** a side chain is depicted as an arm sticking out the hexagon.*

6 ARMS USED FOR SOLAR ENERGY CONVERSION

Important applications of redox ArMs are found in the emerging field of photobiocatalysis [112]. The amount of solar energy that reaches the Earth's surface is orders of magnitude larger than what is available in other forms of renewable energy [113]. Therefore attempts are being made to harvest this energy to perform useful chemical reactions, such as CO_2 reduction [114], [115], C-H bond functionalization [116], or dihydrogen evolution [115], [117]–[119]. Artificial metalloenzymes can be used to perform such

transformations [112], [120]. Photobiocatalytical systems can be prepared with natural systems, such as the existing light-harvesting machinery present in naturally phototrophic organisms to perform photobiocatalysis *in vivo,* to drive a chemical reaction [121]. Furthermore, naturally photoactive enzymes [122] or existing bio-enzymes that show altered activity upon irradiation (*e.g.,* NAD(P)H-using enzymes, as their cofactor is redox-active under irradiation [123]), can be employed to prepare photobiocatalytic systems. These systems can also be prepared by the introduction of artificial cofactors in a "natural" or *de novo* protein backbone. For instance, an artificial or natural enzyme can be driven by an external photosensitizer, directly or *via* a mediator [112], [120], [124]–[126]. It is rather complex to gain a complete understanding of all the different ways by which natural enzymes tune the redox potentials of the different components of the system to optimize electron transfer [127]. However, suboptimal electron transfer and substrate turnover rates in ArMs can lead to unwanted side reactions resulting in the formation of ROS and free radicals, which limits the stability of the enzyme [112], [125].

To optimize electron transfer between different components of the system one can consider an ArM in terms of its different coordination spheres [125]. The metal centre of the catalyst is directly coordinated by ligands, which may be imine (His), thiol (Cys), thioester (Met), or carboxylate (Asp, Glu) residues from the protein, forming the first coordination sphere [125], [128], [129]. The first coordination sphere has a strong impact on the redox potential and thus the reactivity of the metal. When an ArM is prepared using an artificial metal complex coordinated in a protein backbone, tuning of the first coordination sphere is not only realised by deciding on the nature of the coordinating atoms bound to the metal centre: in addition, the geometry of the first coordination sphere can have a strong effect on the electronic and catalytic properties of the ArM. The preferred oxidation state of the metal can be influenced by the nature and geometry of the 1st coordination sphere: hard ligands, such as glutamate or aspartic acid, allow reaching higher oxidation states than softer ligands, such as histidine or cysteine, and the stronger the electron-donating ability of the chosen ligand the lower the oxidation potential becomes [125], [130], [131].

One can also fine-tune the second coordination sphere, which consists of the residues located in the immediate environment around the metal centre. This requires consideration of hydrogen bonding, the presence of charged ligands surrounding the catalyst binding site, the hydrophobicity of the

binding site, or pi-stacking interactions [125], [129], [132]–[137]. Finally, longer ranged interactions can influence the structural features of the binding site or impact the solvent environment of the catalyst and with that impact the redox potential and reactivity of the catalyst [125], [135], [137]–[140].

7 WATER SPLITTING WITH ARMS

Artificial metalloenzymes aimed at producing dihydrogen have been developed both using repurposed proteins fitted with non-native metal ions or complexes, and bias-switched hydrogenases [36], [81]. For example cobaloximes, which show good dihydrogen evolution activity but poor water solubility, have been incorporated into protein scaffolds such as flavodoxin or ferredoxin to afford good ArMs for proton reduction [141], [142]. In ferredoxin electron transfer was observed from a covalently linked ruthenium photosensitizer *via* the native [2Fe-2S] cluster to the cobalt catalyst. A more prolific route consisted of the inclusion of cobalt protoporphyrin IX (CoPPIX), which has dihydrogen evolution activity but suffers from low solubility in water, into various haem-binding proteins [115], [117], [118], [143]. Wild type (WT) cytochrome b_{562}, in which CoPPIX was coordinated by histidine and methionine, formed an efficient catalyst [118]. The activity could be further improved by mutating the axial methionine into alanine, aspartic acid or glutamic acid [118]. While alanine liberated an axial position on the metal for catalysis, the aspartic acid and glutamic acid variants introduced an additional proton relay. All three mutants showed markedly better dihydrogen evolution activity than the WT [118]. A remarkable quality of CoPPIX, especially compared to hydrogenases, is its tolerance to O_2-rich environments. In anaerobic conditions, the alanine mutant turnover numbers (*TON*) approached 1500 in a constant flow cell, [144], while under air a *TON* of 400 was retained. Porphyrins show potential both as dihydrogen evolution catalysts and as photosensitizers [145], though in both cases their low solubility in water hinders many applications. Zinc protoporphyrin IX (ZnPPIX) has been incorporated in human serum albumin to improve its qualities as a photosensitizer. The resulting ArM was able to drive dihydrogen evolution catalysed by Pt-nanoparticles *via* methyl viologen, which served as electron relay [146]. Taking it one step further, Pt-nanoparticles incorporated in the 24-subunit iron storage protein bacterioferritin were able to catalyse dihydrogen evolution using a zinc porphyrin coordinated between bacterioferritin dimers as photosensitizer [147].

Water oxidation, on the other hand, is more challenging for ArMs because of the stress the highly oxidative conditions of the reaction put on the protein scaffold. Still, several attempts have been made: 1) A water oxidation ArM has been prepared from carbonic anhydrase in which the native zinc(II) cofactor has been replaced by iridium(III). The cofactor of carbonic anhydrase is coordinated by three histidine residues and one hydroxide. Replacement of this Zn^{2+} by Ir^{3+} resulted in a WOC which functioned under neutral conditions and had comparable activity to small molecule Ir catalysts in solution [148]. 2) CoPPIX was also used for water oxidation by conjugation to a cytochrome *c* scaffold immobilized on antimony-doped tin oxide. The presence of the protein led to a 6-fold increase in photocurrent density with respect to CoPPIX alone [149]. In short, ArMs that can catalyse water oxidation are scarce and a true photocatalytic water oxidation ArM is yet to be designed.

8 ELECTRON TRANSFER IN PROTEINS

When performing homogeneous photocatalysis with a catalyst embedded in a protein scaffold, electron transfer between the catalyst and photosensitizer is a key step. The rate of electron transfer is controlled by the ability of the PS in solution to approach the protein as well as by the distance over which the electrons need to be transported. In addition, the electron transport rate depends on the medium, *i.e.,* amino acids, internal water, ions, or cofactors through which the electrons have to move. The rate further depends on the redox potentials of the PS, SR, and catalyst, *e.g.,* for a HEC + PS system that operates *via* an oxidative quenching mechanism, the redox potential of the redox couple involving the excited state, $E_{ox}(PS^{+}/PS^{*})$ should be sufficiently higher than that of the catalyst ($E_{red}(Cat/Cat^{-})$ to which an electron is transferred. The distance over which the electron can be transported depends on the charge of the protein and PS as well as on the openness of the binding pocket, since these factors influence the ability of the PS to approach the catalyst in the protein binding pocket. The electron transfer rate k_{ET} (s^{-1}) in the protein is described by Marcus theory according to equation 3 (Fig. 7A) [150], [151]:

$$k_{\mathrm{ET}} = \left[\frac{4\pi^2 H_{\mathrm{AB}}^2}{h(4\pi\lambda RT)^{0.5}}\right] \exp\left[-\frac{(\Delta G^0+\lambda)^2}{4\lambda RT}\right] \qquad 3$$

The H_{AB} (J mol^{-1}) term represents the electronic coupling between the redox centres A=PS* (donor) and B=Cat (acceptor), which depends on the donor-

acceptor distance as well as the medium through which the electron is transferred, λ (J mol^{-1}) is the reorganization energy, h (J s) is the Planck constant, R (J mol^{-1} K^{-1}) is the gas constant, T (K) is the temperature, and ΔG^0 (J mol^{-1}) is the Gibbs free energy of the electron transfer reaction, hence the thermodynamic driving force of the reaction, which is a function of the difference between the electron donor and the acceptor midpoint potential (E_m (V)). The midpoint potential is defined as the potential at which half of a given compound is oxidized and half is reduced.

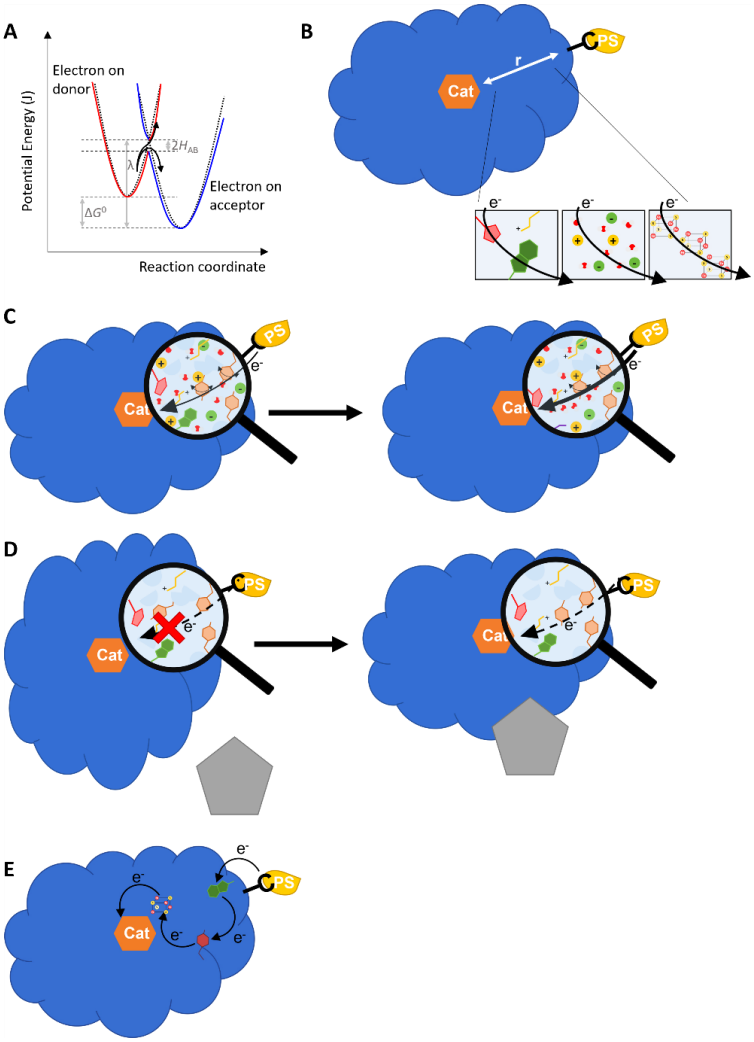

*Figure 7: **A** Parabolic potential energy surfaces for electron transfer from a donor A (**red**) to an acceptor B (**blue**) following Marcus theory. **B** Electron transfer over a distance r through different media that an electron may encounter in a protein. **C** An increased electron transfer rate, represented by a thicker arrow, may result from reorganization (via mutation) of the protein. **D** Gated electron transfer: when electron transfer is impossible in absence of a chemical interacting with the protein (grey pentagon) but becomes possible upon binding of the cofactor. **E** Electron transfer by hole hopping. In all cases the protein scaffold is shown in blue, the catalyst in orange and the photosensitizer in yellow.*

Electron transfer can thus be controlled in the protein *via* tuning of the redox potentials of the donor and acceptor, as discussed above for artificial metalloproteins. This control can be exerted by the protein scaffold *via* gated or coupled electron transfer, and *via* control of the H_{AB} and λ parameters [150]–[153]. Starting with H_{AB}, the medium through which the electron is transferred in a protein is a combination of (post-translationally modified) amino acids and the space between them as well as water, ions, and other cofactors, like the [FeS] clusters in some hydrogenases as mentioned above (Fig. 7B). In general, increasing the atomic packing density increases $k_{ET,}$ while increasing the number of jumps through space reduces k_{ET}. The dynamics inside a protein can impact this parameter by reducing the space that needs to be traversed. λ represents the changes between the starting and final states of the electron transfer process in terms of changes to bond lengths and atom locations in the donor A and acceptor B and the associated changes in the surrounding medium. λ can be influenced by mutations in the protein that influence the geometric constraints and solvent exposure levels experienced by the donor or acceptor sites (Fig. 7C). Gated or coupled electron transfer generally involves an event that is a prerequisite before electron transfer can take place *e.g.,* binding of redox partners or a conformational change in the protein upon binding of a signal molecule (Fig. 7D).

Electron tunnelling through amino acid residues as discussed before does not require their reduction or oxidation, instead the protein functions as a semiconductive matrix. However, amino acids can be reversibly oxidized and reduced to allow electron or hole transfer via a hopping mechanism that can significantly accelerate k_{ET} by offering intermediate points to which transfer can take place, thus reducing the distance between A and B (Fig. 7E) [154], [155]. Hole hopping requires amino acids to be present that have biologically accessible redox potentials, in the order of 1 V vs. NHE or less. Typically, heterocyclic aromatic amino acids like tryptophan or tyrosine play this role.[151], [153], [155] Such amino acids, or cofactors, are capable of forming a redox-active relay over which electron transfer can take place over larger distances through the protein.

9 PROTEIN STABILITY UNDER OXIDATIVE OR REDUCTIVE STRESS

Stability is not often thoroughly investigated for catalytically active ArMs, while in redox enzymes oxidation or reduction of amino acids may have a major impact on the protein. In natural systems, the formation of ROS is in part prevented by optimizing the different metal centres for efficient electron transfer, and in part by an extended "defence" system consisting of multiple proteins and cofactors capable of repair and replacement of damaged proteins, as discussed above for PSII. Still, a single protein is not defenceless either. Within proteins such as peroxidases, defence aimed at preventing oxidation in the binding pocket works by directing holes away from the binding pocket. Important amino acid residues coordinated to the catalytically active metal centre would lose their ability to coordinate the metal upon oxidation, which would destroy the catalytically active site. Redirecting oxidative equivalents towards the protein exterior using specific paths of redox-active ligands effectively protects the inner catalytic site. Once located on an exterior residue, the hole can be reduced easily using reducing equivalents from the aqueous medium around the protein [156], [157].

10 METALLOPROTEIN SCAFFOLDS EMPLOYED IN THIS THESIS

The majority of the artificial metalloenzymes investigated in this thesis have been designed using the dative coordination of a native metalloenzyme to a synthetic metal-based catalyst or photosensitizer. This has been accomplished by first removing the natural cofactor (typically a haem) and followed by the introduction of a synthetic metal complex which bound to the haem-binding pocket of the protein scaffold.

In this thesis three proteins have been used as a scaffold for the preparation of ArMs: myoglobin from *Equus caballus* (Mb), cytochrome b_5 from *Bos taurus* (CB5), and haem acquisition system A from *Pseudomonas aeruginosa* (HasAp) (Fig. 8, 9, 10). All three are metalloproteins that naturally coordinate a haem cofactor and therefore have a sufficiently large binding pocket to axially coordinate non-native metal complexes.

10.1 Myoglobin (Mb)

Myoglobin (Fig. 8) is a mobile oxygen-transporting protein found in the sarcoplasm, where it plays an important role in keeping a constant dioxygen pressure [158]. It binds a haem cofactor directly using one axial histidine, and indirectly (via a water molecule) to a second histidine called the “distal” histidine. In this work myoglobin from equine skeletal muscle was used (Mb, PDB ID 5D5R [159]), which contains 11 histidines. Mb is an alpha-helical protein, consisting of 7 helices. Loss of the haem-cofactor leads to minimal unfolding, which may be advantageous for its stability when coordinating a non-native cofactor [160]. Myoglobin is a commercially available, relatively stable protein that has been used in various studies of ArMs [117], [126], [161], [162].

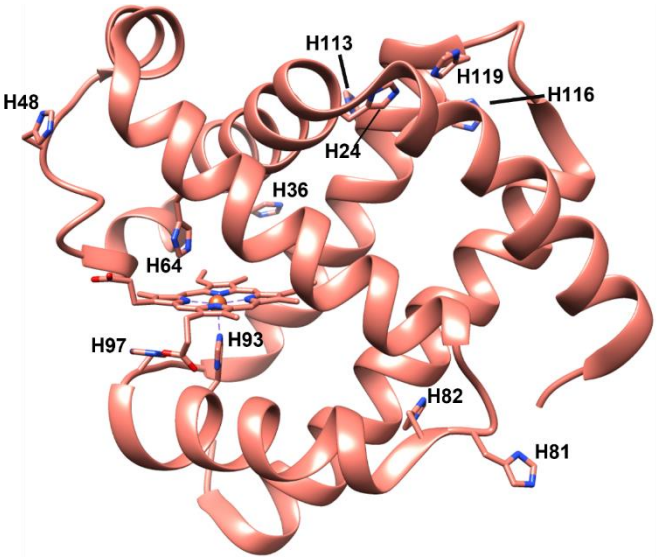

Figure 8: Myoglobin with each of its histidines and haem explicitly shown. PDB ID 5D5R [158].

10.2 Cytochrome b_5 (CB5)

Cytochrome b_5 (CB5, Fig. 9) is a small electron transfer protein that is involved in many different cellular processes. Among others, it interacts with cytochrome P450 [163], cytochrome *c*, myoglobin, cytochrome b_5 reductase, and haemoglobin [164]. CB5 comes in three forms. Microsomal and outer mitochondrial both consist of a soluble fragment and a hydrophobic tail that attaches the protein to the membrane, while a soluble form of cytochrome

b_5 has been found in human erythrocytes [165]. In this work, the soluble fraction of bovine cytochrome b_5 was obtained by expression in *Escherichia coli (E.coli)*. Bovine CB5 (PDB ID 1CYO [166]) consists of 6 alpha-helices surrounding a core of 4 beta-sheets. CB5 contains 5 histidines in total, 2 of which are involved in the coordination of its native haem ligand. It coordinates this haem bi-axially in its binding pocket, which is relatively solvent exposed. Upon loss of haem the majority of the alpha helices are lost, while the beta-sheet core of the protein remains intact (PDB ID of *Rattus norvegicus apo*CB5 1I87 [167]) [168]. CB5 has not been used much as a scaffold for artificial metalloenzymes, though its haem has been exchanged for porphyrins with different metal centres [169]. Due to its small size and relatively open binding pocket CB5 may form a convenient scaffold to contain a catalyst.

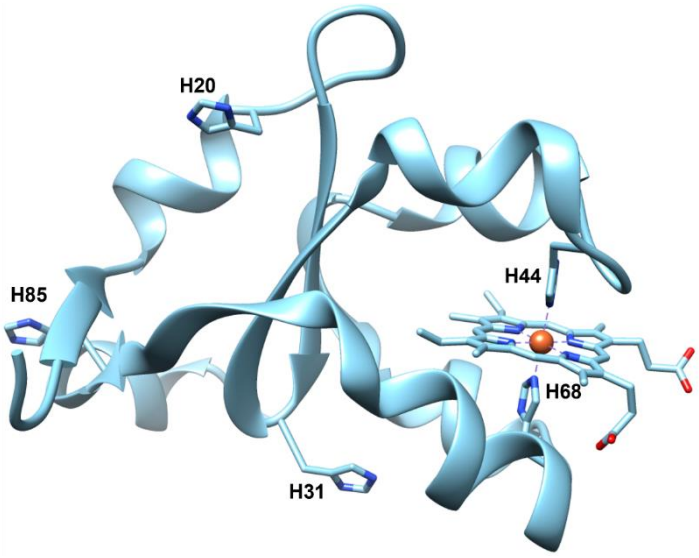

Figure 9: CB5 with each with of its histidines and haem explicitly shown. PDB ID 1CYO [166].

10.3 Haem acquisition system A from *Pseudomonas aeruginosa* (HasAp)

Haem acquisition system A from *Pseudomonas aeruginosa* or HasAp (Fig. 10, PDB ID 3ELL [138]) is a soluble transient haem-binding protein involved in

stealing haem from haemoglobin in a host organism infected by *Pseudomonas aeruginosa*. HasAp is excreted *via* an ABC-transporter to catch haem, which it can then pass on to membrane protein HasR for transport into the cell. HasAp consists of 3 alpha helices that lie against 7 beta sheets. The haem-binding pocket sticks out from there and consists of 2 more loops, coordinating haem bi-axially with a tyrosine and a histidine ligand. HasAp contains 5 histidines in total. The haem-bound (*holo)* protein is in the so-called closed conformation, and the haem-free (*apo*) protein is in the open conformation (PDB ID 3MOK [170]) in which the histidine-containing loop has moved outward. HasAp has been previously shown to bind various non-native ligands [100], [171] to inhibit its native function, showing its potential for binding a non-native metal catalyst.

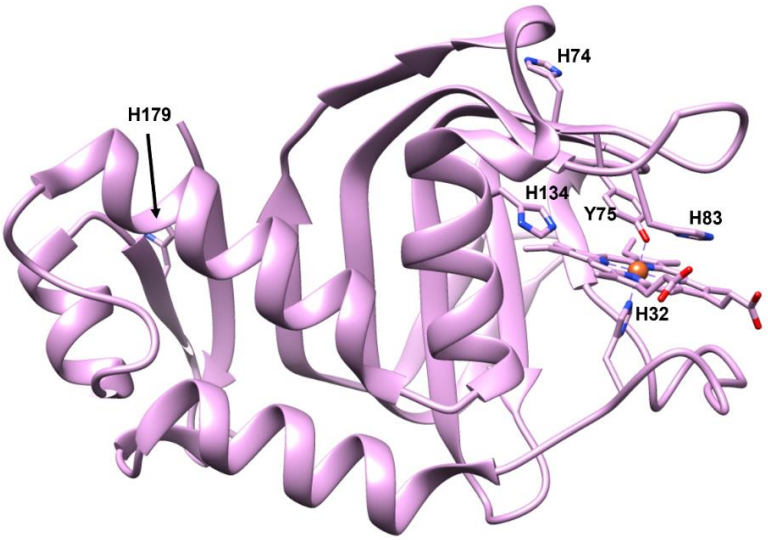

Figure 10: HasAp with each with of its histidines, its coordinating tyrosine ligand and haem explicitly shown. PDB ID 3ELL [170].

11 CATALYST AND PHOTOSENSITIZER COMPLEXES EMPLOYED IN THIS THESIS

Several water oxidation catalysts (WOC) or WOC precursors, dihydrogen evolution catalysts (HEC) or HEC precursors, and several photosensitizers (PS), were considered in this thesis as building blocks for the preparation of ArMs. They are briefly described below.

11.1 WO catalysts

11.1.1 Co-based WOCs

Cobalt(II) phthalocyanine (**1**, Fig. 11) is a first-row WOC deprived of axial ligands in the solid state that is slightly larger than haem [172]. Although its size may make its incorporation into proteins difficult, phthalocyanine compounds with various metal ion centres have been previously incorporated in proteins [100], [173]. **1** is believed to retain its tetradentate ligands upon binding to a protein scaffold. This ligand may play an active role in the water oxidation mechanism, and notably it may serve as a reservoir of electron in oxidation reactions, even when the reaction is metal-centred.

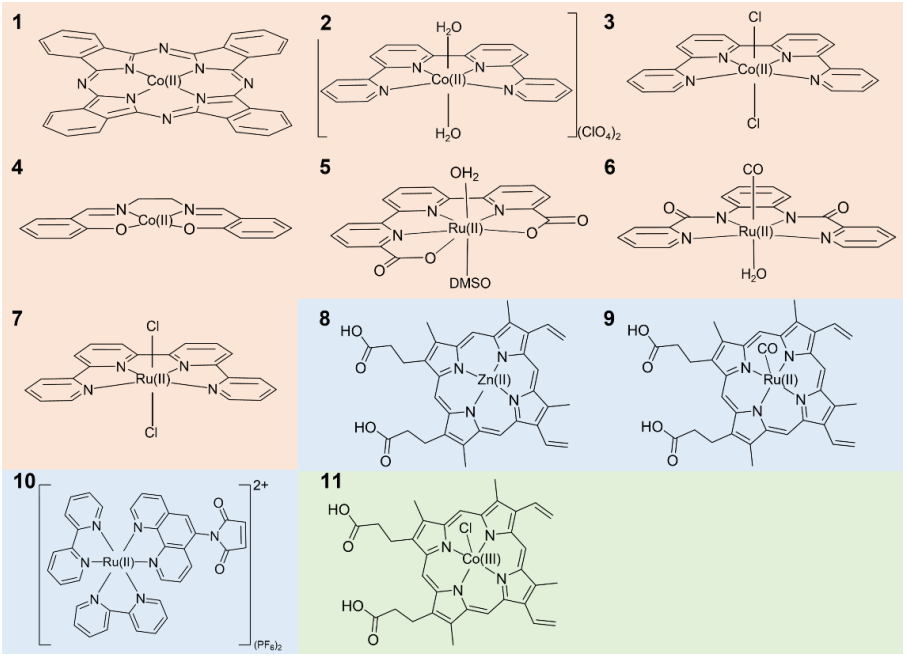

*Figure 11: The chemical structures of water oxidation catalysts (**1**-**7**, orange background), photosensitizers (**8**-**10**, blue background), and the water reduction catalyst (**11**, green background) used in this thesis.*

Two cobalt(II) quarterpyridine complexes have also been selected: $[Co^{II}(qpy)(OH_2)_2](ClO_4)_2$ (**2**, qpy = 2,2':6',2'':6'',2'''-quarterpyridine, Fig. 11) and its precursor $[Co^{II}(qpy)Cl_2]$ (**3**, Fig. 11) [174]. **2** has poor water solubility, while **3** is water soluble. **2** was shown to have catalytic activity for the water oxidation reaction in photochemical conditions using $[Ru(bpy)_3]^{2+}$ as PS and $Na_2S_2O_8$ as SA. In addition, dihydrogen evolution activity under

photochemical conditions was demonstrated using $[Ir^{III}(dF(CF_3)ppy)_2(dtbbpy)]^+$ (HdF(CF_3)ppy = 2-(2,4-difluorophenyl)-5-trifluoromethylpyridine, dtbbpy = 4,4'-di-tert-butyl-2,2'-bipyridine) as the PS and triethanolamine (TEOA) as the sacrificial donor (SD) . The identity of the catalytically active species when Co-based WOCs or HECs such as **2** or **3** are used is a heavily discussed point in the field of photocatalysis. In oxidative conditions ligand oxidation of the metal complex can lead to dissociation of the ligand from the metal and to the formation of cobalt oxide nanoparticles which show good WO activity [175], [176]. Similarly, in reductive conditions the metal centre might be reduced to Co(0), upon which the ligand dissociates and the metal forms catalytically active cobalt nanoparticles.[177], [178] However, **2** was not reported to form nanoparticles when it was used either as HEC or as WOC [174], making it an attractive candidate for incorporation into a protein scaffold. The *TON* (in terms of the [PS]) for dihydrogen evolution was 1730 under >420 nm irradiation of a 7.5 µM solution of **2** in aqueous acetonitrile solution (30% H_2O) with 0.2 M TEOA as SD and 0.03 mM $[Ir^{III}(dF(CF_3)ppy)_2(dtbbpy)]^+$ as PS and 25 mM *p*-cyanoanilinium tetrafluoroborate as proton donor at 23 °C after 20 h. For water oxidation the *TON* was 335 (in terms of the [WOC]) under 457 nm irradiation of a 0.2 µM **2**, 5 mM $Na_2S_2O_8$, 128 µM $Ru(bpy)_3Cl_2$ solution in 15 mM borate buffer pH 8.0 at 23 °C under argon after 1.5 h.

[N,N'-bis(salicylidene)ethane-1,2-diaminato]cobalt(II), also called CoSalen (**4**, Fig. 11) is a reasonably soluble in water. It is a mononuclear precursor for CoO/CoOH nanoparticles that are catalytically active for the water oxidation reaction [179]. The activity of **4** was tested photocatalytically using $[Ru(bpy)_3]^{2+}$ as photosensitizer and $Na_2S_2O_8$ as sacrificial acceptor. The formed nanoparticles were found to give a high *TON* of 854 and a quantum yield of ~0.39 when catalysis was performed with 2.4 µM **4**, 1.0 mM $Ru(bpy)_3(ClO_4)_2$, 5.0 mM $Na_2S_2O_8$ in 80 mM sodium borate buffer at pH 9.0 with >420 nm at room temperature. Due to its small size, we hypothesized that **4** would be easily incorporated into a protein scaffold, as comparable cobalt complexes have been found capable of doing so [100], [171], [180].

11.1.2 Ru-based WOCs

While cobalt has the advantage of being an earth-abundant metal that interacts well with nitrogen ligands in proteins, ruthenium complexes have a rich (photo)chemistry. Though they can access formal oxidation states ranging from -III to +VIII [181], they are mostly found in the oxidation state +II and +III in aqueous solutions. Due to its larger ionic radius octahedral Ru

complexes may transiently coordinate a 7th ligand in the first coordination sphere. Ruthenium complexes bearing tetradentate ligands in their basal plane and coordinated axially to two histidine residues may still be able to perform water oxidation [58], [182].

The ruthenium complex [Ru^{II}(tda-*κ*-N^3O)(DMSO)(OH_2^{ax})] (**5**, H_2tda = [2,2′:6′,2″terpyridine]-6,6″-dicarboxylic acid, Fig. 11) is a precursor to the active water oxidation catalyst: [Ru^{II}(tda-κ-N^3O)($py)_2$] (py = pyridine) [58], [172]. Depending on the oxidation state of the ruthenium centre, the tda^{2-} ligand might be bound to ruthenium via 4 or 5 of its heteroatoms. In the +II oxidation state for example, one of the 2 carboxylates remains uncoordinated, thus becoming "dangling" in aqueous solution. During water oxidation, this dangling carboxylic acid group can stabilize the peroxo intermediate formed in the WNA mechanism, which promotes proton abstraction and accelerates the catalytic reaction [58]. This is in principle advantageous for a protein-coordinated WOC, as it appears much more convenient to perform water oxidation *via* a mononuclear WNA mechanism than via the I2M mechanism, which would require two proteins to come close from each together to allow bimolecular reaction.

The complex [Ru(bpb)(CO)(OH_2)] (**6**, H_2bpb = N,N′-1,2-phenylene-bis(2-pyridine-carboxamide, Fig. 11) is an inactive by-product formed during water oxidation by the [Ru^{III}(bpb)($pic)_2$]Cl WOC (pic = 4-picoline) [183]. The difference between these two complexes, which directly leads to the loss of activity for **6**, is their axial ligands. When using **6** to make an ArM, the axial CO and OH_2 ligands may be replaced by histidines, which are chemically similar to monocyclic nitrogen-containing ring compounds, such as pyridine. The activity of the bis-picoline complex in the WOC has been tested using [Ru($bpy)_3$]($PF_6)_3$ as chemical oxidant. A *TON* of 200 was observed in 0.1 M NaPi pH 7.2, with 30 μM [Ru^{III}(bpb)($pic)_2$]Cl, 3.0 μmol Ru($bpy)_3$($PF_6)_3$ after 7 h. The mechanism of the WOC is believed to be mononuclear [183].

Finally, the complex [Ru^{II}(qpy)Cl_2] (**7**, Fig. 11) has the same open quaterpyridine planar ligands than **2** and **3**, which in principle may allow coordination of a 7th ligand to ruthenium during the catalytic cycle [184]. **7** is also a precursor: upon replacing its axial chloride ligands by pyridines, a catalytically active species was obtained. Here as well axial coordination of histidine residues from a protein may produce a catalytically active species. The active catalyst is formed by the oxidation of the planar quaterpyridine ligand to form 1,1′′′-dioxide-2,2′:6′,2′′:6′′,2′′′quaterpyridine (Fig. 12). This species has a *TON* of up to 2100 using Ce^{IV}-driven chemical water oxidation

depending on the axial ligands. The catalyst concentration was 25 µM in the presence of 247 mM $(NH_4)_2Ce(NO_3)_6$ at 25 °C after 30 min [184].

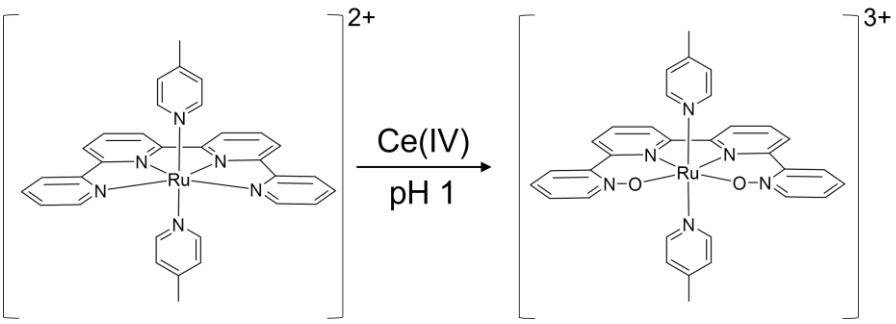

Figure 12: The oxidation of the [Ru^{II}(qpy)py$_2$] (py=pyridine) quarterpyridine ligands to 1,1'''-dioxide-2,2':6',2'':6'',2'''quaterpyridine using $(NH_4)_2Ce(NO_3)_6$ (Ce(IV)) at pH 1 [181].

11.2 Photosensitizers

Next to the water oxidation catalysts three different metal-based photosensitizers have been conjugated with two protein scaffolds in this thesis: zinc(II) protoporphyrin IX, ruthenium(II) protoporphyrin IX, and $[Ru(bpy)_2(1\text{-}(1,10\text{-phenanthrolin-5-yl})\text{-}1H\text{-pyrrole-2,5-dione}](PF_6)_2$ (**8**-**10**, see Fig. 11). As discussed above, porphyrin-based metal compounds can function both as photosensitizers and as dihydrogen evolution catalysts, although low solubility in water hinders their application in homogeneous (photo)catalysis [118], [145]. **10** is a derivative of the commonly used $[Ru(bpy)_3]Cl_2$ complex, in which one of the bipyridyl ligands was functionalized with a maleimide group that allowed covalent linking to cysteine residues [185]. **10** is the only complex of the series that was covalently linked to the protein in this thesis.

11.3 Dihydrogen evolution catalysts

Only one dihydrogen evolution catalyst was used in this work, namely cobalt(III) protoporphyrin IX (**11,** Fig. 11) [117]. CoPPIX in 200 mM Tris-HCl and 100 mM NaCl at pH 7 was reported to give a *TON* of 120 using 1 mM $[Ru(bpy)_3]Cl_2$ as the photosensitizer and 100 mM sodium ascorbate as SD after 8 h. When conjugated to Mb under the same conditions **11** showed a significantly higher *TON* (518), in part due to the improved solubilization of the catalyst [117].

12 ARTIFICIAL PHOTOSYNTHESIS OR PHOTOCATALYSIS

Light-driven reactions can be divided into photocatalytic processes, in which light energy is used to overcome an energy barrier, and photosynthetic processes, in which energy is stored in the reaction products [186]. Fig. 13A shows the schematic Z-scheme of the water oxidation system used in Chapter 3. Here, the potential of the $S_2O_8^{2-}$ SA lies above that of water, so that $\Delta G>0$: this is therefore considered artificial photosynthesis. Fig. 13B shows the Z-scheme for the dihydrogen evolution reaction described in more detail in Chapter 4. Here the energy level of the sacrificial electron donor, TEOA, lies below that of the reaction product (H_2), so that $\Delta G>0$: this reaction is therefore considered artificial photosynthesis also.

Table 1: the redox potentials of the redox couples shown in Fig. 13, defined at pH 7.0.

Redox couple	**Redox potential (V vs. NHE)**	**Reference**
$TEOA^+/TEOA$	0.82	[187]
$ZnPPIX^{+\bullet}/ZnPPIX$	~0.9*	[188], [194]–[196]
$ZnPPIX^{+\bullet}/ZnPPIX^*$	~-0.8*	[188], [194]–[196]
$MV^{2+}/MV^{+\bullet}$	-0.43	[189]
$2H^++2e^-/H_2$	-0.41	[190], [197]
$O_2+H^++4e^-/2H_2O$	0.82	[191], [197]
$Ru(bpy)_3^{3+}/Ru(bpy)_3^{2+}$	1.26	[198]
$Ru(bpy)_3^{3+}/^*Ru(bpy)_3^{2+}$	-0.86	[198]
$Na_2S_2O_8/SO_4^{2-}+SO_4^{-\bullet}$	0.6	[199]

*Approximation based on the ZnPPIX bound to cytochrome *c* or myoglobin

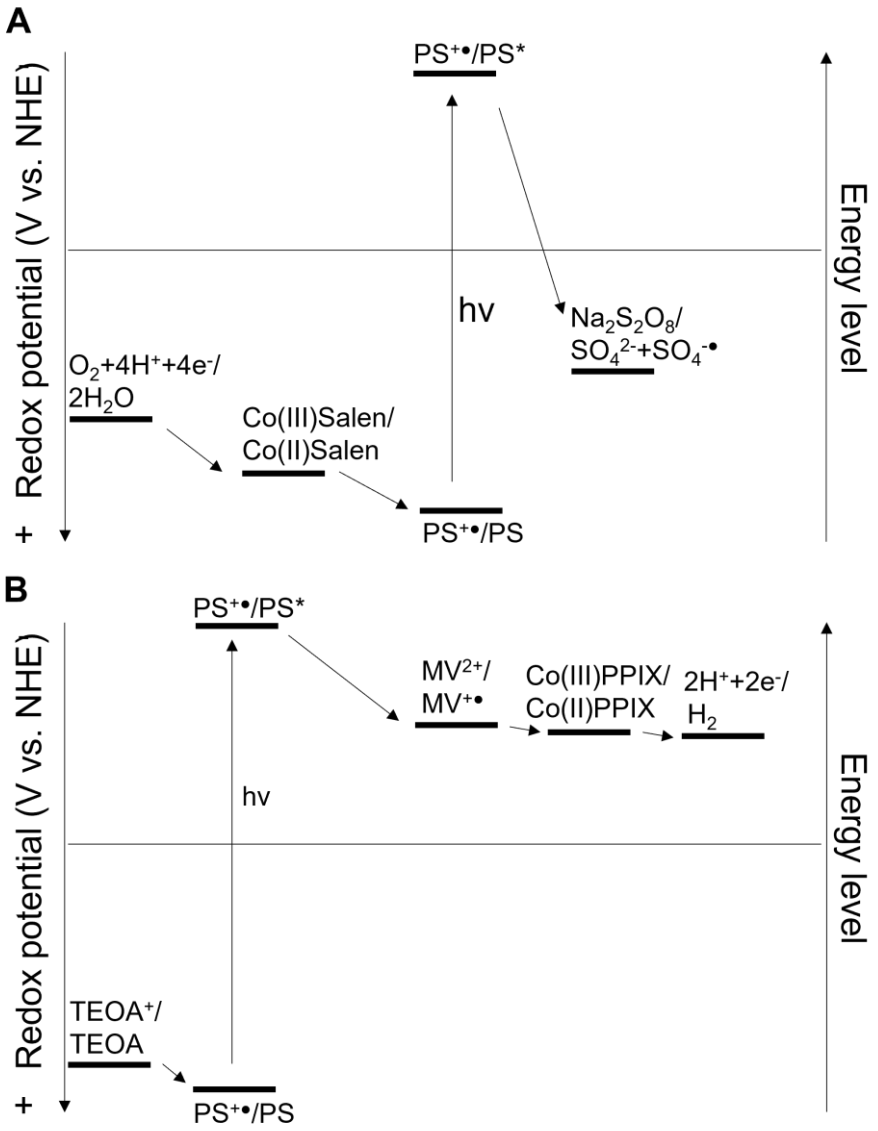

*Figure 13: Schematic of the z-scheme of the water oxidation system in Chapter 3, with CB5:CoSalen as WOC, $Ru(bpy)_3^{2+}$ as PS, and $Na_2S_2O_8$, in **A**. The Z-scheme of the H_2 evolution system used in Chapter 4, with Mb:CoPPIX as HEC, HasAp:RuPPIX or HasAp:ZnPPIX as PS, MV^{2+} as electron relay, and TEOA as SD, in **B.** The relative energy levels, where reasonable values could be found, were from the following literature sources: TEOA* [187], *ZnPPIX* [188],

MV^{2+} [189]*, H^+* [190]*, H_2O* [191]*, $Ru(bpy)_3^{2+}$* [192]*, and $Na_2S_2O_8$* [193] *and are shown in Table 1.*

13 SCOPE OF THIS THESIS

With this thesis, I aim to combine the strengths of synthetic metal-based catalysts, *e.g.,* clear structure to function relationship and a broad range of catalysed reactions, with that of proteins as metal-binding ligands, *e.g.,* selectivity and ability to operate under mild conditions, to prepare artificial metalloenzymes with proton reduction or water oxidation activity. Simultaneously, an effort was made to shed light on the fate of the ArMs after photocatalysis, and hence on the decomposition processes occurring during the photocatalytic reactions. In **Chapter 2**, a semi-native gel electrophoresis method is introduced as a screening method for detecting the binding of cobalt- and ruthenium-based water oxidation catalysts to three types of haem proteins. One of the most promising combinations found was that of cytochrome b_5 (CB5) and CoSalen, where H_2Salen = N,N'-bis(salicylidene)ethylenediamine. In **Chapter 3**, the artificial metalloprotein CB5:CoSalen was explored for its ability to perform photocatalytic water oxidation. *Apo*- and *holo*CB5 were reacted with CoSalen in different protein:catalyst ratios. The water-oxidation activity of the ArMs was tested and the stability of the proteins during the reaction was analysed in detail. In **Chapter 4**, the two other proteins examined in Chapter 2, haem acquisition system Ap (HasAp) and myoglobin (Mb), were used as scaffolds for conjugation of a small-molecule photosensitizer (**8**-**10**) and a dihydrogen evolution catalyst (**11**). The photosensitizing ArM consisting of ZnPPIX or RuPPIX bound to HasAp was used to drive protein-based dihydrogen evolution catalyst Mb-CoPPIX using methyl viologen as an electron relay. Two systems in which HasAp hosted the CoPPIX HEC were also prepared; a mixture consisting of HasAp-ZnPPIX as PS and HasAp-CoPPIX as HEC, and a system in which both catalyst and PS were bound to HasAp, CoPPIX-HasAp-RuPPIX. The catalytic activity of all four systems was tested and compared. Further, the condition of the ArMs was analysed in all systems before and after photocatalysis. In **Chapter 5**, four cysteine mutations were introduced in CB5 for attachment of photosensitizer **10**. The four ArMs based on these four mutants were then used to investigate light-induced electron transfer from the photosensitizer to the haem of CB5. This work identified the optimal position of the ruthenium photosensitizer to drive fast intramolecular photoinduced electron transfer. In the future, such an ArM may be combined

with a catalyst attached by coordination in the haem-binding position, to obtain a bimetallic ArM that combines light absorption, electron transfer, and catalysis.

14 REFERENCES

[1] S. Solomon, G.-K. Plattner, R. Knutti, and P. Friedlingstein, "Irreversible climate change due to carbon dioxide emissions," *Proceedings of the National Academy of Sciences*, vol. 106, no. 6, pp. 1704–1709, Feb. 2009, doi: 10.1073/pnas.0812721106.

[2] P. T. Aakko-Saksa, C. Cook, J. Kiviaho, and T. Repo, "Liquid organic hydrogen carriers for transportation and storing of renewable energy – Review and discussion," *Journal of Power Sources*, vol. 396, pp. 803–823, Aug. 2018, doi: 10.1016/j.jpowsour.2018.04.011.

[3] Q.-L. Zhu and Q. Xu, "Liquid organic and inorganic chemical hydrides for high-capacity hydrogen storage," *Energy Environ. Sci.*, vol. 8, no. 2, pp. 478–512, 2015, doi: 10.1039/C4EE03690E.

[4] P. Preuster, C. Papp, and P. Wasserscheid, "Liquid Organic Hydrogen Carriers (LOHCs): Toward a Hydrogen-free Hydrogen Economy," *Acc. Chem. Res.*, vol. 50, no. 1, pp. 74–85, Jan. 2017, doi: 10.1021/acs.accounts.6b00474.

[5] A. B. Gallo, J. R. Simões-Moreira, H. K. M. Costa, M. M. Santos, and E. Moutinho dos Santos, "Energy storage in the energy transition context: A technology review," *Renewable and Sustainable Energy Reviews*, vol. 65, pp. 800–822, Nov. 2016, doi: 10.1016/j.rser.2016.07.028.

[6] X. Fang, S. Kalathil, and E. Reisner, "Semi-biological approaches to solar-to-chemical conversion," *Chemical Society Reviews*, vol. 49, no. 14, pp. 4926–4952, 2020.

[7] H. Arakawa *et al.*, "Catalysis Research of Relevance to Carbon Management: Progress, Challenges, and Opportunities," *Chem. Rev.*, vol. 101, no. 4, pp. 953–996, Apr. 2001, doi: 10.1021/cr000018s.

[8] T. Jafari, E. Moharreri, A. S. Amin, R. Miao, W. Song, and S. L. Suib, "Photocatalytic Water Splitting—The Untamed Dream: A Review of Recent Advances," *Molecules*, vol. 21, no. 7, 2016, doi: 10.3390/molecules21070900.

[9] J. K. Hurst, "In Pursuit of Water Oxidation Catalysts for Solar Fuel Production," *Science*, vol. 328, no. 5976, pp. 315–316, Apr. 2010, doi: 10.1126/science.1187721.

[10] S. W. Gersten, G. J. Samuels, and T. J. Meyer, “Catalytic oxidation of water by an oxo-bridged ruthenium dimer,” *Journal of the American Chemical Society*, vol. 104, no. 14, pp. 4029–4030, 1982.

[11] F. Liu, J. J. Concepcion, J. W. Jurss, T. Cardolaccia, J. L. Templeton, and T. J. Meyer, “Mechanisms of water oxidation from the blue dimer to photosystem II,” *Inorganic Chemistry*, vol. 47, no. 6, pp. 1727–1752, 2008.

[12] J. K. Hurst, J. L. Cape, A. E. Clark, S. Das, and C. Qin, “Mechanisms of water oxidation catalyzed by ruthenium diimine complexes,” *Inorganic chemistry*, vol. 47, no. 6, pp. 1753–1764, 2008.

[13] U. Hintermair, S. M. Hashmi, M. Elimelech, and R. H. Crabtree, “Particle formation during oxidation catalysis with Cp* iridium complexes,” *Journal of the American Chemical Society*, vol. 134, no. 23, pp. 9785–9795, 2012.

[14] D. J. Vinyard, G. M. Ananyev, and G. Charles Dismukes, “Photosystem II: the reaction center of oxygenic photosynthesis,” *Annual review of biochemistry*, vol. 82, pp. 577–606, 2013.

[15] R. Matheu *et al.*, “Intramolecular Proton Transfer Boosts Water Oxidation Catalyzed by a Ru Complex,” *J. Am. Chem. Soc.*, vol. 137, no. 33, pp. 10786–10795, Aug. 2015, doi: 10.1021/jacs.5b06541.

[16] L. Duan *et al.*, “A molecular ruthenium catalyst with water-oxidation activity comparable to that of photosystem II,” *Nature chemistry*, vol. 4, no. 5, pp. 418–423, 2012.

[17] T. M. Bricker and L. K. Frankel, “The structure and function of CP47 and CP43 in photosystem II,” *Photosynthesis research*, vol. 72, pp. 131–146, 2002.

[18] P. Mulo, C. Sicora, and E.-M. Aro, “Cyanobacterial psbA gene family: optimization of oxygenic photosynthesis,” *Cellular and Molecular Life Sciences*, vol. 66, pp. 3697–3710, 2009.

[19] F. Müh and A. Zouni, “Structural basis of light-harvesting in the photosystem II core complex,” *Protein Science*, vol. 29, no. 5, pp. 1090–1119, 2020.

[20] J. M. Keough, A. N. Zuniga, D. L. Jenson, and B. A. Barry, “Redox control and hydrogen bonding networks: Proton-coupled electron transfer reactions and tyrosine Z in the photosynthetic oxygen-evolving complex,” *The Journal of Physical Chemistry B*, vol. 117, no. 5, pp. 1296–1307, 2013.

[21] Y. Umena, K. Kawakami, J.-R. Shen, and N. Kamiya, “Crystal structure of oxygen-evolving photosystem II at a resolution of 1.9 Å,” *Nature*, vol. 473, no. 7345, pp. 55–60, 2011.

[22] A.-M. A. Hays, I. R. Vassiliev, J. H. Golbeck, and R. J. Debus, “Role of D1-His190 in proton-coupled electron transfer reactions in photosystem II: a chemical complementation study,” *Biochemistry*, vol. 37, no. 32, pp. 11352–11365, 1998.

[23] F. Rappaport, M. Guergova-Kuras, P. J. Nixon, B. A. Diner, and J. Lavergne, “Kinetics and pathways of charge recombination in photosystem II,” *Biochemistry*, vol. 41, no. 26, pp. 8518–8527, 2002.

[24] B. Svensson, C. Etchebest, P. Tuffery, P. Van Kan, J. Smith, and S. Styring, “A model for the photosystem II reaction center core including the structure of the primary donor P680,” *Biochemistry*, vol. 35, no. 46, pp. 14486–14502, 1996.

[25] G. C. Dismukes *et al.*, “Development of bioinspired Mn4O4− cubane water oxidation catalysts: lessons from photosynthesis,” *Accounts of Chemical Research*, vol. 42, no. 12, pp. 1935–1943, 2009.

[26] A. Pinnola, “The rise and fall of Light-Harvesting Complex Stress-Related proteins as photoprotection agents during evolution,” *Journal of Experimental Botany*, vol. 70, no. 20, pp. 5527–5535, 2019.

[27] G. Krause, C. Vernotte, and J.-M. Briantais, “Photoinduced quenching of chlorophyll fluorescence in intact chloroplasts and algae. Resolution into two components,” *Biochimica et Biophysica Acta (BBA)-Bioenergetics*, vol. 679, no. 1, pp. 116–124, 1982.

[28] W. Marulanda Valencia and A. Pandit, “Photosystem II subunit S (PsbS): a nano regulator of plant photosynthesis,” *Journal of Molecular Biology*, p. 168407, Dec. 2023, doi: 10.1016/j.jmb.2023.168407.

[29] J. Dasgupta, G. M. Ananyev, and G. C. Dismukes, “Photoassembly of the water-oxidizing complex in photosystem II,” *Coordination chemistry reviews*, vol. 252, no. 3–4, pp. 347–360, 2008.

[30] D. Godde, H. Schmitz, and M. Weidner, “Turnover of the D-1 reaction center polypeptide from photosystem II in intact spruce needles and spinach leaves,” *Zeitschrift für Naturforschung C*, vol. 46, no. 3–4, pp. 245–251, 1991.

[31] V. M. Johnson and H. B. Pakrasi, “Advances in the Understanding of the Lifecycle of Photosystem II,” *Microorganisms*, vol. 10, no. 5, p. 836, 2022.

[32] J. Yu and P. Takahashi, “Biophotolysis-based hydrogen production by cyanobacteria and green microalgae,” *Communicating current research and educational topics and trends in applied microbiology*, vol. 1, pp. 79–89, 2007.

[33] E. S. Andreiadis, M. Chavarot-Kerlidou, M. Fontecave, and V. Artero, “Artificial Photosynthesis: From Molecular Catalysts for Light-driven Water Splitting to Photoelectrochemical Cells,” *Photochemistry and photobiology*, vol. 87, no. 5, pp. 946–964, 2011.

[34] K. Bolatkhan, B. D. Kossalbayev, B. K. Zayadan, T. Tomo, T. N. Veziroglu, and S. I. Allakhverdiev, “Hydrogen production from phototrophic microorganisms: reality and perspectives,” *international journal of hydrogen energy*, vol. 44, no. 12, pp. 5799–5811, 2019.

[35] T. Yagi and Y. Higuchi, “Studies on hydrogenase,” *Proceedings of the Japan Academy, Series B*, vol. 89, no. 1, pp. 16–33, 2013.

[36] C. Esmieu, P. Raleiras, and G. Berggren, “From protein engineering to artificial enzymes–biological and biomimetic approaches towards sustainable hydrogen production,” *Sustainable Energy & Fuels*, vol. 2, no. 4, pp. 724–750, 2018.

[37] M. W. W. Adams, L. E. Mortenson, and J.-S. Chen, “Hydrogenase,” *Biochimica et Biophysica Acta (BBA) - Reviews on Bioenergetics*, vol. 594, no. 2, pp. 105–176, 1980, doi: https://doi.org/10.1016/0304-4173(80)90007-5.

[38] C. Greening *et al.*, “Genomic and metagenomic surveys of hydrogenase distribution indicate H2 is a widely utilised energy source for microbial growth and survival,” *The ISME journal*, vol. 10, no. 3, pp. 761–777, 2016.

[39] P. M. Vignais and B. Billoud, “Occurrence, Classification, and Biological Function of Hydrogenases: An Overview,” *Chem. Rev.*, vol. 107, no. 10, pp. 4206–4272, Oct. 2007, doi: 10.1021/cr050196r.

[40] J. Noth *et al.*, “[FeFe]-Hydrogenase with Chalcogenide Substitutions at the H-Cluster Maintains Full H2 Evolution Activity,” *Angewandte Chemie*, vol. 128, no. 29, pp. 8536–8540, 2016.

[41] S. Kruse, T. Goris, M. Wolf, X. Wei, and G. Diekert, “The NiFe hydrogenases of the tetrachloroethene-respiring Epsilonproteobacterium Sulfurospirillum multivorans: biochemical studies and transcription analysis,” *Frontiers in Microbiology*, vol. 8, p. 444, 2017.

[42] E. Reijerse *et al.*, “Asymmetry in the Ligand Coordination Sphere of the [FeFe] Hydrogenase Active Site Is Reflected in the Magnetic Spin Interactions of the Aza-Propanedithiolate Ligand,” *The Journal of Physical Chemistry Letters*, vol. 2019, Oct. 2019, doi: 10.1021/acs.jpclett.9b02354.

[43] J. A. Birrell *et al.*, “Spectroscopic and Computational Evidence that [FeFe] Hydrogenases Operate Exclusively with CO-Bridged Intermediates,” *J. Am. Chem. Soc.*, vol. 142, no. 1, pp. 222–232, Jan. 2020, doi: 10.1021/jacs.9b09745.

[44] L. A. Flanagan and A. Parkin, “Electrochemical insights into the mechanism of NiFe membrane-bound hydrogenases,” *Biochemical Society Transactions*, vol. 44, no. 1, pp. 315–328, 2016.

[45] J. H. Artz, O. A. Zadvornyy, D. W. Mulder, P. W. King, and J. W. Peters, “Chapter Eight - Structural Characterization of Poised States in the Oxygen Sensitive Hydrogenases and Nitrogenases,” in *Methods in Enzymology*, vol. 595, S. S. David, Ed., Academic Press, 2017, pp. 213–259. doi: 10.1016/bs.mie.2017.07.005.

[46] H. Ogata, W. Lubitz, and Y. Higuchi, “Structure and function of [NiFe] hydrogenases,” *The Journal of Biochemistry*, vol. 160, no. 5, pp. 251–258, Nov. 2016, doi: 10.1093/jb/mvw048.

[47] G. Huang *et al.*, “The atomic-resolution crystal structure of activated [Fe]-hydrogenase,” *Nature Catalysis*, vol. 2, no. 6, pp. 537–543, Jun. 2019, doi: 10.1038/s41929-019-0289-4.

[48] C. Wang, Z. Lai, G. Huang, and H.-J. Pan, “Current State of [Fe]-Hydrogenase and Its Biomimetic Models,” *Chemistry – A European Journal*, vol. 28, no. 57, p. e202201499, Oct. 2022, doi: 10.1002/chem.202201499.

[49] R. K. Thauer, “The Wolfe cycle comes full circle,” *Proceedings of the National Academy of Sciences*, vol. 109, no. 38, pp. 15084–15085, Sep. 2012, doi: 10.1073/pnas.1213193109.

[50] W. Lubitz, H. Ogata, O. Rüdiger, and E. Reijerse, “Hydrogenases,” *Chem. Rev.*, vol. 114, no. 8, pp. 4081–4148, Apr. 2014, doi: 10.1021/cr4005814.

[51] Y. Nicolet, A. L. de Lacey, X. Vernède, V. M. Fernandez, E. C. Hatchikian, and J. C. Fontecilla-Camps, “Crystallographic and FTIR Spectroscopic Evidence of Changes in Fe Coordination Upon Reduction of the Active Site of the Fe-Only Hydrogenase from Desulfovibrio desulfuricans,” *J. Am. Chem. Soc.*, vol. 123, no. 8, pp. 1596–1601, Feb. 2001, doi: 10.1021/ja0020963.

[52] G. Berggren *et al.*, “Biomimetic assembly and activation of [FeFe]-hydrogenases,” *Nature*, vol. 499, no. 7456, pp. 66–69, Jul. 2013, doi: 10.1038/nature12239.

[53] A. Silakov, B. Wenk, E. Reijerse, and W. Lubitz, “14N HYSCORE investigation of the H-cluster of [FeFe] hydrogenase: evidence for a

nitrogen in the dithiol bridge," *Physical Chemistry Chemical Physics*, vol. 11, no. 31, pp. 6592–6599, 2009.

[54] C. Sommer *et al.*, "Proton Coupled Electronic Rearrangement within the H-Cluster as an Essential Step in the Catalytic Cycle of [FeFe] Hydrogenases," *J. Am. Chem. Soc.*, vol. 139, no. 4, pp. 1440–1443, Feb. 2017, doi: 10.1021/jacs.6b12636.

[55] X. Yang and M. B. Hall, "Monoiron Hydrogenase Catalysis: Hydrogen Activation with the Formation of a Dihydrogen, Fe−Hδ−···Hδ+−O, Bond and Methenyl-H4MPT+ Triggered Hydride Transfer," *J. Am. Chem. Soc.*, vol. 131, no. 31, pp. 10901–10908, Aug. 2009, doi: 10.1021/ja902689n.

[56] A. R. Finkelmann, H. M. Senn, and M. Reiher, "Hydrogen-activation mechanism of [Fe] hydrogenase revealed by multi-scale modeling," *Chemical Science*, vol. 5, no. 11, pp. 4474–4482, 2014.

[57] T. Hiromoto, E. Warkentin, J. Moll, U. Ermler, and S. Shima, "The Crystal Structure of an [Fe]-Hydrogenase–Substrate Complex Reveals the Framework for H2 Activation," *Angewandte Chemie International Edition*, vol. 48, no. 35, pp. 6457–6460, Aug. 2009, doi: 10.1002/anie.200902695.

[58] R. Matheu, M. Z. Ertem, C. Gimbert-Suriñach, X. Sala, and A. Llobet, "Seven Coordinated Molecular Ruthenium–Water Oxidation Catalysts: A Coordination Chemistry Journey," *Chem. Rev.*, vol. 119, no. 6, pp. 3453–3471, Mar. 2019, doi: 10.1021/acs.chemrev.8b00537.

[59] M. D. Karkas, O. Verho, E. V. Johnston, and B. Åkermark, "Artificial photosynthesis: molecular systems for catalytic water oxidation," *Chemical reviews*, vol. 114, no. 24, pp. 11863–12001, 2014.

[60] C. Liu, D. van den Bos, B. den Hartog, D. van der Meij, A. Ramakrishnan, and S. Bonnet, "Ligand controls the activity of light-driven water oxidation catalyzed by nickel (II) porphyrin complexes in neutral homogeneous aqueous solutions," *Angewandte Chemie International Edition*, vol. 60, no. 24, pp. 13463–13469, 2021.

[61] R. Matheu *et al.*, "The development of molecular water oxidation catalysts," *Nature Reviews Chemistry*, vol. 3, no. 5, pp. 331–341, 2019.

[62] S. Ye, C. Ding, M. Liu, A. Wang, Q. Huang, and C. Li, "Water oxidation catalysts for artificial photosynthesis," *Advanced Materials*, vol. 31, no. 50, p. 1902069, 2019.

[63] B. Limburg, E. Bouwman, and S. Bonnet, "Molecular water oxidation catalysts based on transition metals and their decomposition pathways," *Coordination Chemistry Reviews*, vol. 256, no. 15–16, pp. 1451–1467, 2012.

[64] T. Liu, B. Zhang, and L. Sun, “Iron-Based Molecular Water Oxidation Catalysts: Abundant, Cheap, and Promising,” *Chemistry–An Asian Journal*, vol. 14, no. 1, pp. 31–43, 2019.

[65] S. C. Silver, J. Niklas, P. Du, O. G. Poluektov, D. M. Tiede, and L. M. Utschig, “Protein delivery of a Ni catalyst to photosystem I for light-driven hydrogen production,” *Journal of the American Chemical Society*, vol. 135, no. 36, pp. 13246–13249, 2013.

[66] K. G. Kottrup, S. D’Agostini, P. H. van Langevelde, M. A. Siegler, and D. G. Hetterscheid, “Catalytic activity of an iron-based water oxidation catalyst: substrate effects of graphitic electrodes,” *ACS catalysis*, vol. 8, no. 2, pp. 1052–1061, 2018.

[67] D. S. Nesterov and O. V. Nesterova, “Polynuclear cobalt complexes as catalysts for light-driven water oxidation: A review of recent advances,” *Catalysts*, vol. 8, no. 12, p. 602, 2018.

[68] P. Comte, M. K. Nazeeruddin, F. P. Rotzinger, A. J. Frank, and M. Grätzel, “Artificial analogues of the oxygen-evolving complex in photosynthesis: the oxo-bridged ruthenium dimer L2 (H2O) RuIII-O-RuIII (H2O) L2, L= 2, 2’-bipyridyl-4, 4’-dicarboxylate,” *Journal of molecular catalysis*, vol. 52, no. 1, pp. 63–84, 1989.

[69] J. Van Houten and R. J. Watts, “Effect of ligand and solvent deuteration on the excited state properties of the tris (2, 2’-bipyridyl) ruthenium (II) ion in aqueous solution. Evidence for electron transfer to solvent,” *Journal of the American Chemical Society*, vol. 97, no. 13, pp. 3843–3844, 1975.

[70] A. Mazzeo, S. Santalla, C. Gaviglio, F. Doctorovich, and J. Pellegrino, “Recent progress in homogeneous light-driven hydrogen evolution using first-row transition metal catalysts,” *Inorganica Chimica Acta*, vol. 517, p. 119950, 2021.

[71] J. Corredor, M. J. Rivero, C. M. Rangel, F. Gloaguen, and I. Ortiz, “Comprehensive review and future perspectives on the photocatalytic hydrogen production,” *Journal of Chemical Technology & Biotechnology*, vol. 94, no. 10, pp. 3049–3063, 2019.

[72] M. Z. Rahman, M. G. Kibria, and C. B. Mullins, “Metal-free photocatalysts for hydrogen evolution,” *Chemical Society Reviews*, vol. 49, no. 6, pp. 1887–1931, 2020.

[73] M. Wang, Y. Na, M. Gorlov, and L. Sun, “Light-driven hydrogen production catalysed by transition metal complexes in homogeneous systems,” *Dalton Transactions*, no. 33, pp. 6458–6467, 2009.

[74] K. Kalyanasundaram and M. Grätzel, “Light induced redox reactions of water soluble porphyrins, sensitization of hydrogen generation from

water by zincporphyrin derivatives," *Helvetica Chimica Acta*, vol. 63, no. 2, pp. 478–485, 1980.

[75] K. Kalyanasundaram, "Photochemistry and sensitized evolution of hydrogen from water using water-soluble cationic porphyrins. Tetrakis (trimethylaminophenyl) porphyrinatozinc and its free base," *Journal of the Chemical Society, Faraday Transactions 2: Molecular and Chemical Physics*, vol. 79, no. 9, pp. 1365–1374, 1983.

[76] K. Degtyarenko, "Metalloproteins," *Encyclopedia of Genetics, Genomics, Proteomics and Bioinformatics*, 2004.

[77] K. Vong, I. Nasibullin, and K. Tanaka, "Exploring and adapting the molecular selectivity of artificial metalloenzymes," *Bulletin of the Chemical Society of Japan*, vol. 94, no. 2, pp. 382–396, 2021.

[78] K. Faber, *Biotransformations in organic chemistry: a textbook*, no. 660.634 F334B. Springer, 2011.

[79] K. Yamamura and E. T. Kaiser, "Studies on the oxidase activity of copper (II) carboxypeptidase A," *Journal of the Chemical Society, Chemical Communications*, no. 20, pp. 830–831, 1976.

[80] M. E. Wilson and G. M. Whitesides, "Conversion of a protein to a homogeneous asymmetric hydrogenation catalyst by site-specific modification with a diphosphinerhodium (I) moiety," *Journal of the American Chemical Society*, vol. 100, no. 1, pp. 306–307, 1978.

[81] F. Schwizer *et al.*, "Artificial Metalloenzymes: Reaction Scope and Optimization Strategies," *Chem. Rev.*, vol. 118, no. 1, pp. 142–231, Jan. 2018, doi: 10.1021/acs.chemrev.7b00014.

[82] W. Ghattas, J.-P. Mahy, M. Réglier, and A. J. Simaan, "Artificial Enzymes for Diels-Alder Reactions," *ChemBioChem*, vol. 22, no. 3, pp. 443–459, Feb. 2021, doi: 10.1002/cbic.202000316.

[83] H. A. Bunzel, J. A. Smith, T. A. Oliver, M. R. Jones, A. J. Mulholland, and R. Anderson, "Photovoltaic enzymes by design and evolution," *bioRxiv*, pp. 2022–12, 2022.

[84] T. R. Ward, "Artificial Enzymes Made to Order: Combination of Computational Design and Directed Evolution," *Angewandte Chemie International Edition*, vol. 47, no. 41, pp. 7802–7803, Sep. 2008, doi: 10.1002/anie.200802865.

[85] H. A. Bunzel, J. L. R. Anderson, and A. J. Mulholland, "Designing better enzymes: Insights from directed evolution," *Current Opinion in Structural Biology*, vol. 67, pp. 212–218, Apr. 2021, doi: 10.1016/j.sbi.2020.12.015.

[86] C. A. Denard, H. Ren, and H. Zhao, “Improving and repurposing biocatalysts via directed evolution,” *Current opinion in chemical biology*, vol. 25, pp. 55–64, 2015.
[87] P. A. Romero and F. H. Arnold, “Exploring protein fitness landscapes by directed evolution,” *Nature Reviews Molecular Cell Biology*, vol. 10, no. 12, pp. 866–876, Dec. 2009, doi: 10.1038/nrm2805.
[88] R. Krämer, “Supramolecular bioinorganic hybrid catalysts for enantioselective transformations,” *Angewandte Chemie International Edition*, vol. 45, no. 6, pp. 858–860, 2006.
[89] T. Ueno *et al.*, “Design of artificial metalloenzymes using non-covalent insertion of a metal complex into a protein scaffold,” *Journal of organometallic chemistry*, vol. 692, no. 1–3, pp. 142–147, 2007.
[90] C. C. James, B. de Bruin, and J. N. H. Reek, “Transition Metal Catalysis in Living Cells: Progress, Challenges, and Novel Supramolecular Solutions,” *Angewandte Chemie International Edition*, vol. n/a, no. n/a, p. e202306645, Jun. 2023, doi: 10.1002/anie.202306645.
[91] J. Steinreiber and T. R. Ward, “Artificial metalloenzymes as selective catalysts in aqueous media,” *Coordination Chemistry Reviews*, vol. 252, no. 5–7, pp. 751–766, 2008.
[92] F. Rosati and G. Roelfes, “Artificial Metalloenzymes,” *ChemCatChem*, vol. 2, no. 8, pp. 916–927, Aug. 2010, doi: 10.1002/cctc.201000011.
[93] A. D. Liang, J. Serrano-Plana, R. L. Peterson, and T. R. Ward, “Artificial metalloenzymes based on the biotin–streptavidin technology: enzymatic cascades and directed evolution,” *Accounts of chemical research*, vol. 52, no. 3, pp. 585–595, 2019.
[94] T. Heinisch and T. R. Ward, “Artificial metalloenzymes based on the biotin–streptavidin technology: challenges and opportunities,” *Accounts of chemical research*, vol. 49, no. 9, pp. 1711–1721, 2016.
[95] S. Colonna and N. Gaggero, “Enantioselective oxidation of sulphides by dioxiranes in the presence of bovine serum albumin,” *Tetrahedron letters*, vol. 30, no. 45, pp. 6233–6236, 1989.
[96] S. Colonna and A. Manfredi, “Catalytic asymmetric Weitz-Scheffer reaction in the presence of bovine serum albumin,” *Tetrahedron letters*, vol. 27, no. 3, pp. 387–390, 1986.
[97] S. Colonna, A. Manfredi, R. Annunziata, and M. Spadoni, “Catalytic asymmetric weitz-scheffer epoxidation promoted by bovine serum albumin. Part II,” *Tetrahedron*, vol. 43, no. 9, pp. 2157–2164, 1987.
[98] S. Colonna, A. Manfredi, and R. Annunziata, “Changes of stereoselectivity and rate in diels-alder reactions by hydrophobic

solvent effects and by bovine serum albumin," *Tetrahedron letters*, vol. 29, no. 27, pp. 3347–3350, 1988.

[99] S. Colona *et al.*, "Asymmetric weitz-scheffer epoxidation promoted by bovine serum albumin: Part III. Highly stereoselective synthesis of optically active epoxynaphthoquimones," *Tetrahedron*, vol. 44, no. 16, pp. 5169–5178, 1988.

[100] C. Shirataki *et al.*, "Inhibition of heme uptake in Pseudomonas aeruginosa by its hemophore (HasAp) bound to synthetic metal complexes," *Angewandte Chemie*, vol. 126, no. 11, pp. 2906–2910, 2014.

[101] K. Oohora, A. Onoda, and T. Hayashi, "Hemoproteins reconstituted with artificial metal complexes as biohybrid catalysts," *Accounts of Chemical Research*, vol. 52, no. 4, pp. 945–954, 2019.

[102] T. Hayashi, Y. Sano, and A. Onoda, "Generation of new artificial metalloproteins by cofactor modification of native hemoproteins," *Israel Journal of Chemistry*, vol. 55, no. 1, pp. 76–84, 2015.

[103] H. M. Key, P. Dydio, D. S. Clark, and J. F. Hartwig, "Abiological catalysis by artificial haem proteins containing noble metals in place of iron," *Nature*, vol. 534, no. 7608, pp. 534–537, 2016.

[104] A. Thiel *et al.*, "An artificial ruthenium-containing β-barrel protein for alkene–alkyne coupling reaction," *Organic & biomolecular chemistry*, vol. 19, no. 13, pp. 2912–2916, 2021.

[105] R. den Heeten, B. K. Muñoz, G. Popa, W. Laan, and P. C. Kamer, "Synthesis of hybrid transition-metalloproteins via thiol-selective covalent anchoring of Rh-phosphine and Ru-phenanthroline complexes," *Dalton Transactions*, vol. 39, no. 36, pp. 8477–8483, 2010.

[106] P. Haquette *et al.*, "Functionalized cationic (η6-arene) ruthenium (II) complexes for site-specific and covalent anchoring to papain from papaya latex. Synthesis, X-ray structures and reactivity studies," *Tetrahedron Letters*, vol. 49, no. 31, pp. 4670–4673, 2008.

[107] N. Madern, B. Talbi, and M. Salmain, "Aqueous phase transfer hydrogenation of aryl ketones catalysed by achiral ruthenium (II) and rhodium (III) complexes and their papain conjugates," *Applied Organometallic Chemistry*, vol. 27, no. 1, pp. 6–12, 2013.

[108] J. R. Carey *et al.*, "A site-selective dual anchoring strategy for artificial metalloprotein design," *Journal of the American Chemical Society*, vol. 126, no. 35, pp. 10812–10813, 2004.

[109] D. K. Garner, L. Liang, D. A. Barrios, J.-L. Zhang, and Y. Lu, "The important role of covalent anchor positions in tuning catalytic

properties of a rationally designed MnSalen-containing metalloenzyme," *ACS catalysis*, vol. 1, no. 9, pp. 1083–1089, 2011.
[110] Y. Lu, "Design and engineering of metalloproteins containing unnatural amino acids or non-native metal-containing cofactors," *Current opinion in chemical biology*, vol. 9, no. 2, pp. 118–126, 2005.
[111] C. Hu, S. I. Chan, E. B. Sawyer, Y. Yu, and J. Wang, "Metalloprotein design using genetic code expansion," *Chemical Society Reviews*, vol. 43, no. 18, pp. 6498–6510, 2014.
[112] L. Schmermund *et al.*, "Photo-Biocatalysis: Biotransformations in the Presence of Light," *ACS Catal.*, vol. 9, no. 5, pp. 4115–4144, May 2019, doi: 10.1021/acscatal.9b00656.
[113] B. Sørensen, "Renewable energy: a technical overview," *Energy Policy*, vol. 19, no. 4, pp. 386–391, 1991.
[114] Y. Deng, S. Dwaraknath, W. O. Ouyang, C. J. Matsumoto, S. Ouchida, and Y. Lu, "Engineering an Oxygen-Binding Protein for Photocatalytic CO2 Reductions in Water," *Angewandte Chemie*, vol. 135, no. 20, p. e202215719, 2023.
[115] G. A. O. Udry *et al.*, "Photocatalytic Hydrogen Production and Carbon Dioxide Reduction Catalyzed by an Artificial Cobalt Hemoprotein," *International journal of molecular sciences*, vol. 23, no. 23, p. 14640, 2022.
[116] Y. Li, B. Yuan, Z. Sun, and W. Zhang, "C–H bond functionalization reactions enabled by photobiocatalytic cascades," *Green Synthesis and Catalysis*, vol. 2, no. 3, pp. 267–274, Aug. 2021, doi: 10.1016/j.gresc.2021.06.001.
[117] D. JosepháSommer and M. DavidáVaughn, "Protein secondary-shell interactions enhance the photoinduced hydrogen production of cobalt protoporphyrin IX," *Chemical Communications*, vol. 50, no. 100, pp. 15852–15855, 2014.
[118] D. J. Sommer, M. D. Vaughn, B. C. Clark, J. Tomlin, A. Roy, and G. Ghirlanda, "Reengineering cyt b562 for hydrogen production: A facile route to artificial hydrogenases," *Biochimica et Biophysica Acta (BBA)-Bioenergetics*, vol. 1857, no. 5, pp. 598–603, 2016.
[119] A. Call *et al.*, "Improved Electro- and Photocatalytic Water Reduction by Confined Cobalt Catalysts in Streptavidin," *ACS Catal.*, vol. 9, no. 7, pp. 5837–5846, Jul. 2019, doi: 10.1021/acscatal.8b04981.
[120] S. H. Lee, D. S. Choi, S. K. Kuk, and C. B. Park, "Photobiocatalysis: activating redox enzymes by direct or indirect transfer of photoinduced electrons," *Angewandte Chemie International Edition*, vol. 57, no. 27, pp. 7958–7985, 2018.

[121] K. Nakamura, R. Yamanaka, K. Tohi, and H. Hamada, “Cyanobacterium-catalyzed asymmetric reduction of ketones,” *Tetrahedron Letters*, vol. 41, no. 35, pp. 6799–6802, 2000.
[122] D. Mersch *et al.*, “Wiring of photosystem II to hydrogenase for photoelectrochemical water splitting,” *Journal of the American Chemical Society*, vol. 137, no. 26, pp. 8541–8549, 2015.
[123] F. Lan *et al.*, “Preparation of hydrophilic conjugated microporous polymers for efficient visible light-driven nicotinamide adenine dinucleotide regeneration and photobiocatalytic formaldehyde reduction,” *ACS Catalysis*, vol. 10, no. 21, pp. 12976–12986, 2020.
[124] J. Kim and C. B. Park, “Shedding light on biocatalysis: photoelectrochemical platforms for solar-driven biotransformation,” *Current Opinion in Chemical Biology*, vol. 49, pp. 122–129, 2019.
[125] P. Hosseinzadeh and Y. Lu, “Design and fine-tuning redox potentials of metalloproteins involved in electron transfer in bioenergetics,” *Biochimica et Biophysica Acta (BBA) - Bioenergetics*, vol. 1857, no. 5, pp. 557–581, May 2016, doi: 10.1016/j.bbabio.2015.08.006.
[126] W. Zhang and F. Hollmann, “Nonconventional regeneration of redox enzymes–a practical approach for organic synthesis?,” *Chemical Communications*, vol. 54, no. 53, pp. 7281–7289, 2018.
[127] R. E. Blankenship *et al.*, “Comparing photosynthetic and photovoltaic efficiencies and recognizing the potential for improvement,” *science*, vol. 332, no. 6031, pp. 805–809, 2011.
[128] A. Bhagi-Damodaran *et al.*, “Why copper is preferred over iron for oxygen activation and reduction in haem-copper oxidases,” *Nature chemistry*, vol. 9, no. 3, pp. 257–263, 2017.
[129] M. R. DuBois and D. L. DuBois, “The roles of the first and second coordination spheres in the design of molecular catalysts for H 2 production and oxidation,” *Chemical Society Reviews*, vol. 38, no. 1, pp. 62–72, 2009.
[130] G. Battistuzzi, M. Bellei, C. A. Bortolotti, and M. Sola, “Redox properties of heme peroxidases,” *Archives of biochemistry and biophysics*, vol. 500, no. 1, pp. 21–36, 2010.
[131] J. Geng, I. Davis, F. Liu, and A. Liu, “Bis-Fe (IV): nature’s sniper for long-range oxidation,” *JBIC Journal of Biological Inorganic Chemistry*, vol. 19, pp. 1057–1067, 2014.
[132] J. A. Laureanti *et al.*, “Protein scaffold activates catalytic CO2 hydrogenation by a rhodium bis (diphosphine) complex,” *ACS Catalysis*, vol. 9, no. 1, pp. 620–625, 2018.

[133] L. V. Hale and N. K. Szymczak, “Hydrogen transfer catalysis beyond the primary coordination sphere,” *ACS Catalysis*, vol. 8, no. 7, pp. 6446–6461, 2018.

[134] D. Bansal, G. Kumar, G. Hundal, and R. Gupta, “Mononuclear complexes of amide-based ligands containing appended functional groups: role of secondary coordination spheres on catalysis,” *Dalton Transactions*, vol. 43, no. 39, pp. 14865–14875, 2014.

[135] J. T. Bays *et al.*, “The influence of the second and outer coordination spheres on Rh (diphosphine) 2 CO2 hydrogenation catalysts,” *ACS Catalysis*, vol. 4, no. 10, pp. 3663–3670, 2014.

[136] J. Tang, P. Yao, L. Wang, H. Bian, M. Luo, and F. Huang, “Schiff base complex conjugates of bovine serum albumin as artificial metalloenzymes for eco-friendly enantioselective sulfoxidation,” *RSC advances*, vol. 8, no. 71, pp. 40720–40730, 2018.

[137] L. Leone, M. Chino, F. Nastri, O. Maglio, V. Pavone, and A. Lombardi, “Mimochrome, a metalloporphyrin-based catalytic Swiss knife,” *Biotechnology and Applied Biochemistry*, vol. 67, no. 4, pp. 495–515, 2020.

[138] D. Z. Zee and T. D. Harris, “Enhancing catalytic alkane hydroxylation by tuning the outer coordination sphere in a heme-containing metal–organic framework,” *Chemical Science*, vol. 11, no. 21, pp. 5447–5452, 2020.

[139] M. L. Reback *et al.*, “The role of a dipeptide outer-coordination sphere on H2-production catalysts: influence on catalytic rates and electron transfer,” *Chemistry–A European Journal*, vol. 19, no. 6, pp. 1928–1941, 2013.

[140] S. Sinha and C. K. Williams, “Outer-coordination sphere in multi-H+/multi-e–molecular electrocatalysis,” *Iscience*, vol. 25, no. 1, 2022.

[141] M. Bacchi *et al.*, “Cobaloxime-Based Artificial Hydrogenases,” *Inorg. Chem.*, vol. 53, no. 15, pp. 8071–8082, Aug. 2014, doi: 10.1021/ic501014c.

[142] S. R. Soltau, P. D. Dahlberg, J. Niklas, O. G. Poluektov, K. L. Mulfort, and L. M. Utschig, “Ru–protein–Co biohybrids designed for solar hydrogen production: understanding electron transfer pathways related to photocatalytic function,” *Chemical science*, vol. 7, no. 12, pp. 7068–7078, 2016.

[143] E. H. Edwards, J. Jelušić, S. Chakraborty, and K. L. Bren, “Photochemical hydrogen evolution from cobalt microperoxidase-11,” *Journal of Inorganic Biochemistry*, vol. 217, p. 111384, 2021.

[144] T. Dhanasekaran, J. Grodkowski, P. Neta, P. Hambright, and E. Fujita, “p-Terphenyl-sensitized photoreduction of CO2 with cobalt and iron porphyrins. Interaction between CO and reduced metalloporphyrins,” *The Journal of Physical Chemistry A*, vol. 103, no. 38, pp. 7742–7748, 1999.

[145] K. Ladomenou, M. Natali, E. Iengo, G. Charalampidis, F. Scandola, and A. G. Coutsolelos, “Photochemical hydrogen generation with porphyrin-based systems,” *Coordination Chemistry Reviews*, vol. 304–305, pp. 38–54, Dec. 2015, doi: 10.1016/j.ccr.2014.10.001.

[146] T. Komatsu, R.-M. Wang, P. A. Zunszain, S. Curry, and E. Tsuchida, “Photosensitized Reduction of Water to Hydrogen Using Human Serum Albumin Complexed with Zinc− Protoporphyrin IX,” *Journal of the American Chemical Society*, vol. 128, no. 50, pp. 16297–16301, 2006.

[147] E. R. Clark and D. M. Kurtz, “Photosensitized H 2 generation from ‘one-pot’ and ‘two-pot’ assemblies of a zinc-porphyrin/platinum nanoparticle/protein scaffold,” *Dalton Transactions*, vol. 45, no. 2, pp. 630–638, 2016.

[148] M. Kim and S. Lee, “Catalytic Water Oxidation by Iridium-Modified Carbonic Anhydrase,” *Chemistry–An Asian Journal*, vol. 13, no. 3, pp. 334–341, 2018.

[149] C. Casadevall, H. Zhang, S. Chen, D. J. Sommer, D.-K. Seo, and G. Ghirlanda, “Photoelectrochemical Water Oxidation by Cobalt Cytochrome C Integrated-ATO Photoanode,” *Catalysts*, vol. 11, no. 5, p. 626, 2021.

[150] R. A. Marcus and N. Sutin, “Electron transfers in chemistry and biology,” *Biochimica et Biophysica Acta (BBA)-Reviews on Bioenergetics*, vol. 811, no. 3, pp. 265–322, 1985.

[151] H. R. Williamson, B. A. Dow, and V. L. Davidson, “Mechanisms for control of biological electron transfer reactions,” *Bioorganic chemistry*, vol. 57, pp. 213–221, 2014.

[152] L. J. C. Jeuken, “Conformational reorganisation in interfacial protein electron transfer,” *Biochimica et Biophysica Acta (BBA) - Bioenergetics*, vol. 1604, no. 2, pp. 67–76, Jun. 2003, doi: 10.1016/S0005-2728(03)00026-4.

[153] H. B. Gray and J. R. Winkler, “Electron transfer in proteins,” *Annual review of biochemistry*, vol. 65, no. 1, pp. 537–561, 1996.

[154] J. J. Warren, M. E. Ener, A. Vlček, J. R. Winkler, and H. B. Gray, “Electron hopping through proteins,” *Coordination Chemistry*

Reviews, vol. 256, no. 21, pp. 2478–2487, Nov. 2012, doi: 10.1016/j.ccr.2012.03.032.

[155] J. R. Winkler and H. B. Gray, "Electron flow through biological molecules: does hole hopping protect proteins from oxidative damage?," *Quarterly Reviews of Biophysics*, vol. 48, no. 4, pp. 411–420, 2015, doi: 10.1017/S0033583515000062.

[156] H. B. Gray and J. R. Winkler, "Functional and protective hole hopping in metalloenzymes," *Chemical Science*, vol. 12, no. 42, pp. 13988–14003, 2021.

[157] M. Kathiresan and A. M. English, "LC-MS/MS suggests that hole hopping in cytochrome c peroxidase protects its heme from oxidative modification by excess H 2 O 2," *Chemical science*, vol. 8, no. 2, pp. 1152–1162, 2017.

[158] J. B. Wittenberg and B. A. Wittenberg, "Myoglobin function reassessed," *Journal of Experimental Biology*, vol. 206, no. 12, pp. 2011–2020, Jun. 2003, doi: 10.1242/jeb.00243.

[159] T. R. M. Barends *et al.*, "Direct observation of ultrafast collective motions in CO myoglobin upon ligand dissociation.," *Science*, vol. 350, no. 6259, pp. 445–450, Oct. 2015, doi: 10.1126/science.aac5492.

[160] Y. KAWAMURA-KONISHI, H. KIHARA, and H. SUZUKI, "Reconstitution of myoglobin from apoprotein and heme, monitored by stopped-flow absorption, fluorescence and circular dichroism," *European journal of biochemistry*, vol. 170, no. 3, pp. 589–595, 1988.

[161] M. Ohashi, T. Koshiyama, T. Ueno, M. Yanase, H. Fujii, and Y. Watanabe, "Preparation of artificial metalloenzymes by insertion of chromium (III) Schiff base complexes into apomyoglobin mutants," *Angewandte Chemie International Edition*, vol. 42, no. 9, pp. 1005–1008, 2003.

[162] T. Ueno *et al.*, "Crystal structures of artificial metalloproteins: tight binding of FeIII(Schiff-Base) by mutation of Ala71 to Gly in apo-myoglobin.," *Inorg Chem*, vol. 43, no. 9, pp. 2852–2858, May 2004, doi: 10.1021/ic0498539.

[163] F. P. Guengerich, "On 'Evidence for the participation of cytochrome b5 in hepatic microsomal mixed-function oxidation reactions' by Alfred Hildebrandt and Ronald W. Estabrook," *Archives of Biochemistry and Biophysics*, vol. 726, p. 109177, Sep. 2022, doi: 10.1016/j.abb.2022.109177.

[164] J. B. Schenkman and I. Jansson, "The many roles of cytochrome b5," *Pharmacology & therapeutics*, vol. 97, no. 2, pp. 139–152, 2003.

[165] P. G. Passon, D. W. Reed, and D. E. Hultquist, “Soluble cytochrome b5 from human erythrocytes,” *Biochimica et Biophysica Acta (BBA) - Bioenergetics*, vol. 275, no. 1, pp. 51–61, Jul. 1972, doi: 10.1016/0005-2728(72)90023-0.

[166] R. C. Durley and F. S. Mathews, “Refinement and structural analysis of bovine cytochrome b5 at 1.5 A resolution.,” *Acta Crystallogr D Biol Crystallogr*, vol. 52, no. Pt 1, pp. 65–76, Jan. 1996, doi: 10.1107/S0907444995007827.

[167] C. J. Falzone, M. R. Mayer, E. L. Whiteman, C. D. Moore, and J. T. Lecomte, “Design challenges for hemoproteins: the solution structure of apocytochrome b5.,” *Biochemistry*, vol. 35, no. 21, pp. 6519–6526, May 1996, doi: 10.1021/bi960501q.

[168] W. Pfeil, “Thermodynamics of apocytochrome b5 unfolding,” *Protein Science*, vol. 2, no. 9, pp. 1497–1501, 1993.

[169] J. Ozols and P. Strittmatter, “The interaction of porphyrins and metalloporphyrins with apocytochrome b5,” *J. Biol. Chem*, vol. 239, no. 4, pp. 1018–1023, 1964.

[170] A. Y. Alontaga *et al.*, “Structural characterization of the hemophore HasAp from Pseudomonas aeruginosa: NMR spectroscopy reveals protein-protein interactions between Holo-HasAp and hemoglobin.,” *Biochemistry*, vol. 48, no. 1, pp. 96–109, Jan. 2009, doi: 10.1021/bi801860g.

[171] G. Centola *et al.*, “Gallium(III)–Salophen as a Dual Inhibitor of Pseudomonas aeruginosa Heme Sensing and Iron Acquisition,” *ACS Infect. Dis.*, vol. 6, no. 8, pp. 2073–2085, Aug. 2020, doi: 10.1021/acsinfecdis.0c00138.

[172] J. Chen, P. Luan, C. Ding, and C. Li, “Understanding the factors governing the water oxidation reaction pathway of mononuclear and binuclear cobalt phthalocyanine catalysts,” *Chemical Science*, vol. 13, no. 30, pp. 8797–8803, 2022.

[173] Y. Shisaka *et al.*, “Hijacking the Heme Acquisition System of Pseudomonas aeruginosa for the Delivery of Phthalocyanine as an Antimicrobial,” *ACS Chemical Biology*, vol. 14, no. 7, pp. 1637–1642, 2019.

[174] C.-F. Leung *et al.*, “A cobalt (II) quaterpyridine complex as a visible light-driven catalyst for both water oxidation and reduction,” *Energy & Environmental Science*, vol. 5, no. 7, pp. 7903–7907, 2012.

[175] S. Fukuzumi and D. Hong, “Homogeneous versus heterogeneous catalysts in water oxidation,” *European Journal of Inorganic Chemistry*, vol. 2014, no. 4, pp. 645–659, 2014.

[176] D. Hong *et al.*, "Water-soluble mononuclear cobalt complexes with organic ligands acting as precatalysts for efficient photocatalytic water oxidation," *Energy & Environmental Science*, vol. 5, no. 6, pp. 7606–7616, 2012.

[177] N. Kaeffer, A. Morozan, J. Fize, E. Martinez, L. Guetaz, and V. Artero, "The Dark Side of Molecular Catalysis: Diimine–Dioxime Cobalt Complexes Are Not the Actual Hydrogen Evolution Electrocatalyst in Acidic Aqueous Solutions," *ACS Catal.*, vol. 6, no. 6, pp. 3727–3737, Jun. 2016, doi: 10.1021/acscatal.6b00378.

[178] N. Queyriaux, R. T. Jane, J. Massin, V. Artero, and M. Chavarot-Kerlidou, "Recent developments in hydrogen evolving molecular cobalt(II)–polypyridyl catalysts," *Coordination Chemistry Reviews*, vol. 304–305, pp. 3–19, Dec. 2015, doi: 10.1016/j.ccr.2015.03.014.

[179] S. Fu *et al.*, "A mononuclear cobalt complex with an organic ligand acting as a precatalyst for efficient visible light-driven water oxidation," *Chemical communications*, vol. 50, no. 17, pp. 2167–2169, 2014.

[180] T. Ueno *et al.*, "Coordinated design of cofactor and active site structures in development of new protein catalysts.," *J Am Chem Soc*, vol. 127, no. 18, pp. 6556–6562, May 2005, doi: 10.1021/ja045995q.

[181] L. A. Oro, "Ruthenium Catalysts and Fine Chemistry. Edited by C. Bruneau, P. H. Dixneuf," *Advanced Synthesis & Catalysis*, vol. 347, no. 6, pp. 883–883, May 2005, doi: 10.1002/adsc.200505085.

[182] R. Matheu, J. Benet-Buchholz, X. Sala, and A. Llobet, "Synthesis, structure, and redox properties of a trans-diaqua Ru complex that reaches seven-coordination at high oxidation states," *Inorganic Chemistry*, vol. 57, no. 4, pp. 1757–1765, 2018.

[183] M. D. Kärkäs, T. Åkermark, H. Chen, J. Sun, and B. Åkermark, "A Tailor-Made Molecular Ruthenium Catalyst for the Oxidation of Water and Its Deactivation through Poisoning by Carbon Monoxide," *Angewandte Chemie International Edition*, vol. 52, no. 15, pp. 4189–4193, 2013.

[184] Y. Liu *et al.*, "Catalytic Water Oxidation by Ruthenium (II) Quaterpyridine (qpy) Complexes: Evidence for Ruthenium (III) qpy-N, N'''-dioxide as the Real Catalysts," *Angewandte Chemie*, vol. 126, no. 52, pp. 14696–14699, 2014.

[185] M. Indelli, i C. Bignozzi, A. Harriman, J. Schoonover, and F. Scandola, "Four intercomponent processes in a Ru (II)-Rh (III) polypyridine dyad: Electron transfer from excited donor, electron transfer to excited acceptor, charge recombination, and electronic energy transfer,"

Journal of the American Chemical Society, vol. 116, no. 9, pp. 3768–3779, 1994.

[186] F. E. Osterloh, "Photocatalysis versus photosynthesis: A sensitivity analysis of devices for solar energy conversion and chemical transformations," *ACS Energy Letters*, vol. 2, no. 2, pp. 445–453, 2017.

[187] K. Kalyanasundaram, J. Kiwi, and M. Grätzel, "Hydrogen evolution from water by visible light, a homogeneous three component test system for redox catalysis," *Helvetica Chimica Acta*, vol. 61, no. 7, pp. 2720–2730, 1978.

[188] E. M. Becker, D. R. Cardoso, and L. H. Skibsted, "Quenching of excited states of red-pigment zinc protoporphyrin IX by hemin and natural reductors in dry-cured hams," *European Food Research and Technology*, vol. 232, pp. 343–349, 2011.

[189] S. M. Kim *et al.*, "Reduction-controlled viologen in bisolvent as an environmentally stable n-type dopant for carbon nanotubes," *Journal of the American Chemical Society*, vol. 131, no. 1, pp. 327–331, 2009.

[190] A. Razzaq and S.-I. In, "TiO2 Based Nanostructures for Photocatalytic CO2 Conversion to Valuable Chemicals," *Micromachines*, vol. 10, p. 326, May 2019, doi: 10.3390/mi10050326.

[191] A.-M. Manke, K. Geisel, A. Fetzer, and P. Kurz, "A water-soluble tin (IV) porphyrin as a bioinspired photosensitiser for light-driven proton-reduction," *Physical Chemistry Chemical Physics*, vol. 16, no. 24, pp. 12029–12042, 2014.

[192] T. Koike and M. Akita, "Visible-light radical reaction designed by Ru- and Ir-based photoredox catalysis," *Inorganic Chemistry Frontiers*, vol. 1, no. 8, pp. 562–576, 2014.

[193] S. Yuan, P. Liao, and A. N. Alshawabkeh, "Electrolytic manipulation of persulfate reactivity by iron electrodes for trichloroethylene degradation in groundwater.," *Environ Sci Technol*, vol. 48, no. 1, pp. 656–663, 2014, doi: 10.1021/es404535q.

[194] J. Cowan and H. B. Gray, "Synthesis and properties of metal-substituted myoglobins," *Inorganic Chemistry*, vol. 28, no. 11, pp. 2074–2078, 1989.

[195] N. P. Co, R. M. Young, A. L. Smeigh, M. R. Wasielewski, and B. M. Hoffman, "Symmetrized photoinitiated electron flow within the [Myoglobin: Cytochrome b 5] complex on singlet and triplet time scales: Energetics vs dynamics," *Journal of the American Chemical Society*, vol. 136, no. 36, pp. 12730–12736, 2014.

[196] H. Elias, M. H. Chou, and J. R. Winkler, "Electron-transfer kinetics of zinc-substituted cytochrome c and its Ru (NH3) 5 (histidine-33)

derivative," *Journal of the American Chemical Society*, vol. 110, no. 2, pp. 429–434, 1988.

[197] M. W. Kanan and D. G. Nocera, "In situ formation of an oxygen-evolving catalyst in neutral water containing phosphate and Co2+," *Science*, vol. 321, no. 5892, pp. 1072–1075, 2008.

[198] A. Juris, V. Balzani, F. Barigelletti, S. Campagna, P. Belser, and A. von von Zelewsky, "Ru (II) polypyridine complexes: photophysics, photochemistry, eletrochemistry, and chemiluminescence," *Coordination Chemistry Reviews*, vol. 84, pp. 85–277, 1988.

[199] F. A. Frame *et al.*, "Photocatalytic Water Oxidation with Nonsensitized IrO2 Nanocrystals under Visible and UV Light," *J. Am. Chem. Soc.*, vol. 133, no. 19, pp. 7264–7267, May 2011, doi: 10.1021/ja200144w.